U.S. DEPARTMENT OF THE INTERIOR
U.S. GEOLOGICAL SURVEY

RESPONSE OF U.S. GEOLOGICAL SURVEY CREEPMETERS IN CENTRAL CALIFORNIA TO THE OCTOBER 18, 1989 LOMA PRIETA EARTHQUAKE

By

K.S. Breckenridge[1] and R.W. Simpson[2]

Open-File Report 95-830

1995

[1]retired
[2]USGS, 345 Middlefield Rd., MS 977, Menlo Park, CA 94025

RESPONSE OF U.S. GEOLOGICAL SURVEY CREEPMETERS IN CENTRAL CALIFORNIA TO THE OCTOBER 18, 1989 LOMA PRIETA EARTHQUAKE [1]

By
K.S. Breckenridge and R.W. Simpson

Table of Contents

[1] This report has been submitted to "The Loma Prieta, California, earthquake of October 17, 1989--postseismic effects, aftershocks, and other phenomena: U.S. Geological Survey Professional Paper 1550-D (in preparation)."

RESPONSE OF U.S. GEOLOGICAL SURVEY CREEPMETERS IN CENTRAL CALIFORNIA TO THE OCTOBER 18, 1989 LOMA PRIETA EARTHQUAKE

By K.S. Breckenridge and R.W. Simpson

ABSTRACT

At the time of the Loma Prieta earthquake, eighteen USGS creepmeters in central California recorded coseismic steps ranging in size from -0.35 to 6.8 mm. Five of the closest instruments on the San Andreas fault and three on the Calaveras fault also displayed long-term rate changes in the months after the earthquake. The coseismic steps seem to bear little relation in magnitude or sense to static stress changes calculated using dislocation models of the earthquake rupture, but 1-year average creep rate changes (faster on the San Andreas and slower on the Calaveras) do correlate well with static stress changes. This correlation favors low values of apparent coefficient of friction. Observed advances and deficits in cumulative slip at the closest sites caused by the positive and negative rate changes are in fair agreement with deformation predicted by a 3D dislocation model that requires anomalous slip to extend to depths in excess of 10 km. Rate changes observed at several creepmeters in the years before Loma Prieta may be precursory, but are difficult to interpret unambiguously because they fall in a period of extended drought. A two year period of retarded creep at the Cienega Winery site CWC before the Loma Prieta earthquake contains an interesting interval with normal right-lateral (RL) creep events superposed on unusual left-lateral (LL) background drift. Assuming that this behavior was tectonic in origin and not drought- or instrument-related, it can be explained by stresses imposed from two different sources. One source could be slip on the San Andreas fault below the creepmeter, causing the RL creep events. The second could be slip on the sub-parallel Calaveras fault or other local structures which were caught up in regional tectonic adjustments following the 26 January 1986 Tres Pinos earthquake, causing the LL movement and retarding the cumulative progress of the instrument. In this scenario, the retardation at CWC could have been a precursor to Loma Prieta in the sense that it too was a manifestation of regional tectonic changes that would eventually trigger the Loma Prieta earthquake.

INTRODUCTION

At the time of the Loma Prieta earthquake, twenty-seven U.S. Geological Survey creepmeters were operating within 205 km of the epicenter (Figure 1a). Eighteen of these instruments recorded coseismic steps ranging in size from -0.35 to 6.8 mm, and eight of sites closest to the epicenter displayed significant changes in slip rate in the months after the earthquake (Table 1). For several stations, the Loma Prieta signal is the largest anomaly recorded in up to 25 years of operation. Possible precursory rate changes were observed on several instruments (Breckenridge

and Burford, 1990).

The USGS creepmeters are of several different designs, and data are collected at various intervals ranging from minutes to months depending upon the configuration of a particular instrument (Table 1). Descriptions of the instruments and sites have been published in Schulz and others (1982, 1983) and more recently in Schulz (1989). Eighteen sites are equipped with satellite telemetry that sample the creepmeter every 10 minutes (Silverman and others, 1989), while micrometer dial readings at the remaining 9 sites are taken quarterly.

Additional creepmeters on the San Andreas fault installed by researchers from the University of Colorado are discussed by Behr and others (1990, 19--). Alinement arrays on the Calaveras, Hayward, and other Bay Area faults maintained by researchers at the University of California at San Francisco are also described by Galehouse (1992, 19--).

Numerous instances of triggered slip on fault segments at considerable distances from an earthquake rupture are reported in the literature. For example, such slip occurred after the 1968 Borrego Mountain earthquake (Allen and others, 1972), the 1979 Imperial Valley earthquake (Fuis, 1982; Sieh, 1982), the 1981 Westmorland earthquake (Sharp and others, 1986a), the 1983 Coalinga earthquake (Mavko and others, 1985; Schulz and others, 1987), the 1984 Morgan Hill earthquake (Schulz, 1984), the 1986 Tres Pinos earthquake (Simpson and others, 1988), the 1986 North Palm Springs earthquake (Fagerson and others, 1986; Sharp and others, 1986b, Wesson and others, 1986; Williams and others, 1986, 1988), the 1987 Superstition Hills earthquake (Sharp, 1989; Hudnut and Clark, 1989; McGill and others, 1989), and the 1989 Loma Prieta earthquake (Behr and others, 1990; Galehouse, 1990; McClellan and Hay, 1990).

If the triggered slip persists, it may be difficult to distinguish from afterslip, although traditionally "afterslip" has been used to describe postseismic slip occurring on the same fault that the earthquake occurred on and localized in the rupture region or in its immediate vicinity (e.g., Smith and Wyss, 1968; Scholz and others, 1969; Burford, 1972, 1973; Cohn and others, 1982; Wesson, 1987; Bilham, 1989; Marone and others, 1991).

Some of these triggered responses, especially coseismic steps recorded on creepmeters, are most likely produced by the shaking of fault and instrument during passage of the seismic waves (King and others, 1977; Allen and others, 1972; Fuis, 1982; Williams and others, 1988; McGill and others, 1989). Such shaking probably triggers the release of a backlog of slip that had been held in the Earth's near-surface or in the creepmeter itself by friction. Other longer-term responses, including alterations in creep rate and occasionally in creep direction (e.g., Mavko and others, 1985; Simpson and others, 1988), may be caused by static changes in the stress field produced by the distant earthquake's fault offset. The reality of such static stress changes in the Earth is not in question, because sensitive strainmeters have detected them at great distances from earthquakes (e.g., Johnston and others, 1987; Shimada and others, 1987; Johnston and others, 1990). Microseismicity rate changes on central California faults also appear to correlate with calculated static stress changes after the Loma Prieta earthquake (Reasenberg and Simpson, 1992, 19--), suggesting that these faults can and do react to small stress perturbations at

seismogenic depths.

In the next sections we present data for the eight USGS creepmeters nearest to the Loma Prieta epicenter. One of the largest uncertainties in the interpretation of creepmeter data is introduced by seasonal and rainfall-induced fluctuations. For this reason, rainfall records are also presented and we explore the possible effects of weather on creepmeter behavior. Because tectonic accelerations or retardations in creep rates may occur before certain earthquakes (e.g., Nason, 1973; Burford, 1988), establishing the tectonic as opposed to the rainfall-related significance of creep rate changes is important, although difficult to accomplish (e.g., Gilman and Goulty (1972), Langbein and others (1993)).

We attempt to relate the observed coseismic steps and longer-term creep rate changes that occurred at the time of the Loma Prieta earthquake to static stress changes calculated from simple dislocation models of the rupture in an elastic half-space. To put the Loma Prieta observations into perspective and to improve the statistics, we have compiled creepmeter data for 4 other moderate to large Bay Area earthquakes that occurred before 1989, in addition to the 1990 Chittenden earthquake which was a large aftershock to the Loma Prieta earthquake. The results described below suggest that, although the sense (right-lateral (RL) or left-lateral (LL)) of coseismic steps at creepmeter sites seems to bear little relation to the imposed static shear stress changes, there is a statistically significant relation between the sense (RL or LL) of long-term average creep rate changes and the sign of coseismic shear stress changes. For the Loma Prieta earthquake the magnitudes of these quantities are also well correlated.

We also describe three-dimensional boundary element models used to estimate the total anomalous slip advance or deficit that can be expected at creepmeter sites as a result of the Loma Prieta creep rate changes. The models suggest that under some instruments, complex spatial distributions of stress can exist, and the effects of RL stress changes imposed at the surface might be superseded with time by larger LL stresses imposed at depth. These models suggest that for the 5 creepmeters on the San Andreas fault, cumulative advances ranging from 12-60 mm can be expected as a result of the Loma Prieta earthquake, whereas at the 3 sites on the Calaveras fault, cumulative delays of 6-29 mm might be expected. Although post-Loma Prieta adjustments at all creepmeters are not yet complete, these estimates appear to agree with extrapolations of observed advances or deficits in long-term pre-earthquake trends.

DATA FROM EIGHT CREEPMETERS CLOSEST TO THE EARTHQUAKE

In this paper we concentrate our discussion on the responses of the 8 closest USGS instruments on the San Andreas and Calaveras faults (Figure 1b). Data for all of the operating instruments is available to interested investigators.

Long term data from the five closest instruments on the San Andreas fault are shown in Figure

2a. Data from a 3-year time-window centered about the Loma Prieta earthquake date are displayed in Figure 2b. These plots were made using daily data (1 point per day) selected (for the most part) from 10-minute interval data by an automatic algorithm. These daily data have been adjusted to agree with quarterly micrometer readings where data gaps exist or calibrations are in question. Such adjustments are usually unnecessary or small, and none of the significant variations in creeprate presented here are likely to result from instrument calibration problems.

The most obvious features in the long-term data in Figure 2a are the post-Loma Prieta rate increases at XSJ, XHR, and CWC. Post-seismic changes at XFL and XMR are smaller compared with the other 3 sites and with other variations recorded at those sites over the years. At the bottoms of Figures 2a and 2b, plots of daily rainfall from Paicines, California, located near the fault between creepmeters CWC and XFL, show that the Loma Prieta earthquake occurred during a drought, lasting from 1986 to about 1991.

Figure 3a shows cumulative data for the 3 creepmeters along the Calaveras fault near Hollister. Two traces are plotted for the Shore Road creepmeter: XSH for daily data selected from 10-minute telemetered data, and XSHM for approximately quarterly micrometer measurements to facilitate comparison with quarterly dial readings from Central Avenue (HLC) and D Street (HLD) in Hollister. The most obvious feature is the slip-rate decrease since the Loma Prieta earthquake at all 3 sites. There are indications that this decrease began before the earthquake and may be related to the M5.6 Tres Pinos earthquake on 26 January 1986. These declining slip-rates occur during a period of drought as shown by the plot of daily rainfall from Paicines, which casts some uncertainty on the tectonic significance of these changes. Galehouse (19--) has reported slower creeprates at a number of sites on the Hayward and southern Calaveras faults after the Loma Prieta earthquake.

RAINFALL EFFECTS AND CREEP RETARDATION

Small pre-Loma Prieta rate changes occurred at XHR, CWC, and XMR in the 2-3 years before the earthquake (Figures 2a,b). It is of some interest to know whether these changes are of tectonic origin and could represent precursors to the Loma Prieta earthquake. Burford (1988), for example, discussed the possible significance of retardations in creep rate as precursory signals for local magnitude 4-6 earthquakes. The definition of a creep retardation is subjective, but Table 2 lists possible occurrences of creep retardations before the Loma Prieta earthquake in addition to those tabulated by Burford (1988). As a general rule of thumb we look for rate decreases of at least 30% compared to the long-term average rate, using a duration of at least 12 to 18 months to avoid seasonal effects. By this rule the deficit at XHR in 1988 and 1989 does not qualify as retardation, but we include it anyway given its uniqueness in the data.

Figure 4 depicts creep at each site along the San Andreas fault after extracting an average annual rate, determined by least squares fit. Creep retardation phases defined by Burford (1988) and additional retardations listed in Table 2 are indicated by bars at the top of each creep trace in

Figure 4 to facilitate comparison between periods of slip deficit and lack of precipitation.

The trace at the bottom of Figure 4 represents cumulative rainfall at Paicines after a long-term annual trend of 15.4 inches/year has been removed. Since 1970 two droughts have occurred in California: one from 1976 to 1978 when the average annual rainfall was 8.9 inches/year, and from 1986 to 1991 when the average precipitation was 7.9 inches/year. Data from January 1991 through December 1992 yield a rate of 12.7 inches/year. In this rainfall trace, periods of drought are clearly shown by a downward sloping trend.

Since the Loma Prieta earthquake occurred in the third year of a drought it is important to explore to what extent preseismic and postseismic rate changes may be attributed to lack of rain. Because we have no direct measurements of soil moisture near any of the instruments, we instead compare creep characteristics from the recent drought with those from the prior drought. This comparison is less than optimal given the difference in severity of the two dry spells. Nevertheless it does provide some insight into what type of drought response can be expected.

For example, Figure 3b, focusing on a 6 year window around the Loma Prieta earthquake, shows clearly the correlation of seasonal RL movement at XSH with rainfall. In the 3 years before the quake all 3 creep events occurred during rain, with 2 events decaying LL over several months time. Since the quake, there has been no dextral movement without rainfall. Instead LL movement returns within a few hours of RL onset.

At creepmeter HLC there is a similar seasonal pattern following the quake, in which movement from April to November is essentially flat to slightly LL, while movement from November to April is RL. Indeed dextral slip in the first few months after Loma Prieta may be strongly associated with rainfall. Schulz and others (1982) point out that creepmeter HLD spans only a portion of the fault zone and may record as little as 30% of the overall movement there. This accounts for the lack of apparent correlation with data from HLC and XSH in terms of rate and features in the long-term data. In the 3 years before Loma Prieta the creep rate at HLD is slightly higher than the long-term average: 2.1 mm/yr compared with a least squares rate of 1.5 mm/yr from Schulz et al. (1982). Since October 1989 HLD has recorded LL drift.

Along the San Andreas fault we find a range of creep-rainfall responses. During the 1976-77 drought XSJ and XMR were recording lower than average rates of creep. At XSJ however the deficit continued almost 2 years beyond the return of normal precipitation. At XMR the retardation phase ended at about the same time as the drought, but began 5 or 6 months before reduced rainfall. XSH, on the Calaveras fault, was also slower than normal during the 1976-77 drought. Like XSJ, retardation at XSH continued beyond the end of the drought, lasting until the Coyote Lake earthquake. From 1978 to 1985 precipitation was relatively normal. During this period Burford (1988) identified slip deficits at XSJ (1978-1980, 1983-1988), XHR (1984), XFL (1983-1986), XMR (1983-1986), and XSH (1978-1979, 1982-1984). During the recent drought from 1986 to 1991, retardation at XSJ began ~2.5 years before the drought and ended ~8 months before the drought did. CWC and XHR saw deficits that were entirely within the drought period, terminated by or just before the Loma Prieta earthquake. XSH and HLC, with deficits beginning

in 1986 or 1987, continue to record less slip despite resumption of normal rainfall. XMR comes closest to following recent rainfall fluctuations in that retardation began in 1988 and may have ended in mid-1991, based on faster inter-event slip.

Comparing creep retardation to seismicity, four of five creepmeters on the San Andreas fault display retardations prior to Loma Prieta earthquake (Table 2), with durations ranging from 7 years at XSJ where the deficit lasted until almost 6 months after the quake, to 11 months at XMR where episodic creep events resumed before the quake but the overall rate remained lower than average until almost 2 years later. At XFL the data show no real change before the earthquake, and post-seismic slip is expressed as a surge in February 1990, coincident with rainfall. Post-seismic rates continue to be above the long-term average at XSJ and XHR, though both sites began to slow down in mid- to late-1991. At CWC, XFL, and XMR the rate for 1992 is roughly equivalent to the pre-established average rate.

Although we can point with certainty to creep events at some sites that do correlate with rainfall, and to fairly well defined seasonal behavior patterns at other sites, the correlation of some of the most interesting rate changes with weather and season remains enigmatic. For the 14 occurrences of creep retardation at 6 sites documented by Burford (1988), 4 instances fell completely within drought periods, 3 instances spanned periods of drought and normal rain, and 7 instances occurred during years with normal rainfall. Because the behavior of individual instruments can be idiosyncratic and dependent on local conditions, it is not possible to appeal to the contrary behavior of even nearby sites to answer some of these questions. Our approach in the rest of this paper will be to try to point out where anomalies could arise from weather-related causes even though our preferred explanation is tectonic. In Appendix A we discuss the rainfall related history of several individual instruments in more detail.

COSEISMIC STEPS AND STATIC STRESS CHANGES

Coseismic steps were recorded at the 6 closest USGS creepmeters on the San Andreas and Calaveras faults with sampling intervals short enough (10 minutes) to detect such steps. These "coseismic" responses occurred within 10-20 minutes of the earthquake origin time, the uncertainty in timing being caused by the coarseness of the sampling interval. Table 1 lists coseismic steps at all creepmeters in the network, and Figure 5 shows raw data for the 6 closest instruments.

Figure 6 compares the coseismic steps at the six creepmeters with the calculated Loma Prieta stress changes based on a dislocation model of Lisowski and others (1990) used to match geodetic measurements of coseismic surface displacements. Static stress changes at the creepmeter sites were calculated using equations derived by Okada (1992) for dislocations in an elastic half-space. Coseismic steps could not be inferred for HLC or HLD because these instruments are read manually at quarterly intervals. Of six observed coseismic steps, one (at XFL) is LL and all of the others are RL. No strong relation exists between either sign or magnitude of the steps and

sign or magnitude of the calculated stress changes, especially in view of the tendency of coseismic steps in RL fault systems to occur in a RL sense.

Five earthquakes other than the Loma Prieta with magnitudes greater than 5 have occurred in the region since 1974 (Figure 1b). They are: Thanksgiving Day (M5.1), Coyote Lake (M5.9), Morgan Hill (M6.2), Tres Pinos (M5.3), and Chittenden (M5.4). For all six earthquakes, 4 LL and 17 RL coseismic steps were observed (Table 4, Figure 7). Of the 4 LL steps, two occurred at sites where model calculations predict LL shear stress changes, and two occurred at sites where calculations predict RL shear stress changes. Conversely, at the 6 sites with coseismic steps where LL stress changes are predicted, only 2 showed LL coseismic steps.

These results imply that the sense (RL or LL) of coseismic steps at the six creepmeter sites bears little relation to the imposed static shear stress changes. If we adopt the null hypothesis that the direction of a coseismic step is independent of the sign of imposed static stress change, then a two-sided χ^2 test (e.g., Sachs, 1982) applied to the data displayed in Figures 6 and 7, does not allow us to reject the null hypothesis at even the 50% confidence level. We conclude that the sense of observed coseismic steps bears no obvious strong relation to the calculated static stress changes. Although all but one of the large coseimic steps did occur for RL static stress changes, there was only one instance of a large imposed LL static change, so the geometry of faults and earthquakes in the region has not lent itself to testing the hypothesis in question.

It does appear from visual inspection of Figure 7 that the 26 occurrences of increased RL shear were more likely to have a sizable coseismic step than the 19 occurrences of added LL shear, many of which had a zero step and are not plotted in Figure 7. The larger amplitude and the larger number of RL steps presumably reflects the fact that all of the creepmeters are installed across faults that normally creep in a RL sense.

More often than not, the coseismic step probably reflects the triggered release of a backlog of slip either in the near-surface of the Earth or in the instrument itself by the shaking that accompanies the passage of seismic waves. The magnitude of the dynamic stress changes associated with the passage of seismic waves is, in general, much larger that the magnitude of the static stress changes (Spudich and others, 1993). On a right-lateral fault, such a backlog would normally be right-lateral, although a few sites might have a left-lateral backlog resulting from seasonal variations in slip direction of the instrument caused by rainfall, local soil conditions, and installation configuration. We cannot rule out the possibility that, because of radiation patterns and ground conditions, those sites with RL shear added might also have been the sites that experienced the greater amount of dynamic shaking during the earthquake. Nevertheless, the results shown in Figure 7 suggest that added RL static shear encourages the triggered release of a backlog of slip in a RL system, while added LL static shear can discourage such a triggered release.

Williams and others (1988) suggested that the amount of slip triggered on part of the southern San Andreas fault by the 1986 North Palm Springs earthquake agreed well with the size of the slip deficit at the site. McGill and others (1989) suggested that slip deficit is probably only part of the story, because some sites showed triggered events associated with both the 1989 Elmore

Ranch and Superstition Hills earthquakes, separated by only 11 hours, whereas one might expect the deficit to have been shaken out by the first shock. We looked for a correlation between the magnitude of the coseismic step and the slip deficit at our eight San Andreas and Calaveras sites, where slip deficit is defined as the difference between the long-term rate at a site and the average rate in the 1-year period preceding the earthquake (Figure 8). (The two points in Figure 8 with large negative deficits come from long-term rates before the Chittenden earthquake, an aftershock to the Loma Prieta earthquake; these negative deficits are caused by faster than normal rates at the two sites caused by Loma Prieta afterslip.) Although there is a suggestion that the largest steps correlate with the largest deficits as defined here, the strength of the correlation is not great.

We could find no significant agreement between sign of coseismic steps and sign of 1-year average rate changes (Figure 9). The two-sided Chi-square test did not allow us to reject the null hypothesis that no relation existed with a confidence any greater than 40%. The absence of any such a relation is consistent with the idea that, in most cases, coseismic steps largely reflect the release of a backlog of slip rather than a clean response to newly imposed stress changes, although it is not possible to rule out a combination of the two effects.

CREEP RATE CHANGES AND STATIC STRESS CHANGES

Average 1-year slip rates for the five creepmeters on the San Andreas fault increased at the time of the Loma Prieta earthquake, whereas rates for the three sites on the Calaveras fault decreased (Figures 2,3; Tables 3,4). To compare creeprate changes with calculated static stress changes, three different dislocation models of the Loma Prieta rupture were used based on geometries and slip distributions proposed by Lisowski and others (1990), Marshall and others (1991), and Beroza (1991). Simpson and Reasenberg (Table 1, 1994) tabulate the details of these three Loma Prieta models. For one site, changes in the rupture orientation from model to model changes the sign of calculated shear stress because this site is near a node in the stress field. In general, the stresses calculated at distances of several rupture lengths from the epicenter are comparable model to model.

Figure 10 compares the fractional change in 1-year average creep rates before and after the Loma Prieta earthquake with calculated static stress changes from the three Loma Prieta models. The fractional change in average rate is defined by:

$$\frac{\Delta\bar{V}}{V_0}$$

where $\Delta\bar{V}$ is the change in average rate over the given time window, and V_0 is the average rate before Loma Prieta over the given time window.

In order to see if there was any significant relationship between the signs of the rate changes and the signs of the stress changes, we tested the null hypothesis that these quantities were independent by applying a two-sided χ^2 test to the respective fourfold tables.

For shear stresses, the null hypothesis that the quantities are independent can be rejected at the 99%, 96%, and 83% confidence levels (χ^2 values of 8, 4.4, 1.9) for the Lisowski, Beroza, and Marshall models respectively when the stresses are calculated at the surface. The confidence limits are even better if the stresses are calculated at greater depths (e.g., 10 km) because the horizontal shear stresses change sign under HLC and HLD in the Marshall model (see Figure 15 and Table 6).

For normal stresses, the null hypothesis that the quantities are independent can be rejected at the 0%, 52%, and 96% confidence levels (χ^2 values of 0, 0.5, 4.4) for the Lisowski, Beroza, and Marshall models respectively. The sense of relation for normal stresses suggested by the Marshall model would yield an increase in creep rate in response to negative values of normal stress which, in the convention used here, would imply more compression. If a relation of this sort exists, it would be counter-intuitive given that Coulomb's law predicts greater friction on the fault as a result of greater compression.

We interpret these results to mean that for the 3 models tested, there is a good relation between slip rate change and shear stress change, but that a relation between slip rate change and normal stress change is unlikely.

In an effort to put this relationship on a firmer footing, we repeated the statistical tests using data for four earlier earthquakes and the Chittenden aftershock, as well as for the Loma Prieta earthquake (Table 4). Model ruptures for each earthquake were made using dislocation rectangles positioned and oriented from mainshock and aftershock locations and from focal mechanism information (Table 5). Amounts of slip were assigned to these dislocation surfaces to yield the observed seismic moments. By examining the results of six earthquakes together, we hoped that model-dependent effects would be either made apparent or minimized in the statistics. The data for all 6 earthquakes are shown in Figure 11. For shear stress, there is a relation at the 95% confidence level (χ^2 = 3.88). For normal stress, the null hypothesis of independence cannot be rejected, implying that no strong relation exists.

A slightly sharper result is obtained if the lower calculated values of stress change are discarded. For example, Reasenberg and Simpson (1992, 1994) reported that significant correlations exist between shear stress changes and microseismicity rate changes down to stress levels of about 0.1 bar. If we repeat the statistical tests, eliminating those data points for which the shear stress changes were less than 0.05 bar (Figure 12), then for shear stresses, there is a relation at the 99% confidence level (χ^2 = 6.58). These results are summarized in Table 6.

Similar statistical tests applied to each of the earthquakes individually show that, not unexpectedly, the largest earthquakes (Loma Prieta and Morgan Hill) give the most definitive results. The results of such tests are also dependent upon the choice of averaging interval. We used a 1-year

interval for the tests described above. For a 3-year window, XMR yields a slower average rate after Loma Prieta compared to the rate before, which worsens the statistical results because the calculated static stress changes require an increase in rate at XMR. It would be desirable to discover some objective criterion for choosing the averaging interval, but in the absence of such a criterion perhaps the best that can be done is to try a range of reasonable intervals to demonstrate that any results obtained do not depend strongly on the choice of interval length.

The best overall relationship between fractional 1-year average rate changes and applied static stress changes from Table 6 can be expressed as:

$$\frac{\Delta\bar{V}}{V_0} \approx (8 \text{ bars}^{-1})\, \Delta\tau$$

where $\Delta\tau$ is in bars, although values obtained range from 4 to 9. This is not a very general relationship because it is tied to a 1-year averaging window, but the data on the whole do not seem adequate to support a more complex relation. The data from XHR and CWC might be good enough to warrant a fit to some of the empirical relations described below, but we have not done this.

COEFFICIENT OF APPARENT FRICTION

In correlating microseismicity rate changes with Coulomb failure function changes, Reasenberg and Simpson (1992, 19--) found that the best correlations were obtained for low assumed values of the apparent coefficient of friction μ'. (In the terminology used by Reasenberg and Simpson (19--), the apparent coefficient of friction is the value inferred by neglecting pore fluid pressure changes.) The absence of any significant relationship between creep rate changes and calculated static stress changes reported in the previous section is consistent with a low value of μ'.

As another way to examine this, we correlated the Coulomb stress for different values of μ' with the fractional rate change. Values of correlation coefficient ρ are weakly but systematically peaked at low values of the apparent coefficients of friction μ' (Figure 13). The correlation coefficient ρ improves slightly if we delete all values of Coulomb stress less than 0.05 bars. In both cases the correlations are significant at the 95% confidence level, although the slight differences for neighboring values of μ' in Figure 13 are not likely to be very significant.

CREEP RATE VS. STRESS LAW

It would be very desirable to have a rheological law that would allow us to predict how a creeping fault would respond to applied stresses. The calculated stress distributions discussed in the next section suggest that inferring information about such a law from the response of a single creepmeter to a single earthquake will not be easy.

Nason and Weertman (1973) pointed out that although the geometry of fault creep events requires an upper yield point behavior on the part of the fault gouge, a unique constitutive law cannot be inferred from the shape of the creep events alone. Nonetheless, a number of authors have attempted to infer parameters for various plausible types of creep laws by looking at creep events or afterslip decay.

Crough and Burford (1977) used a power law fault-zone rheology to relate the shapes of individual creep events with stress. The power law is:

$$dU/dt = C\tau^n$$

and the resulting displacement for creep events is given by:

$$U(t) = U_f\left[1 - 1/[Ct(n-1)U_f^{n-1} + 1]^{1/(n-1)}\right]$$

where U(t) is the displacement at time t after the onset of the creep event, τ is the driving stress, U_f is the final displacement, $U_r = U - U_f$ is the remaining displacement, C is a constant of proportionality, and n is the power law exponent. Wesson (1987, 1988) used this law for his discussions of fault dynamics and Bilham (1989) used it to fit afterslip data to the 1987 Superstition Hills, California earthquake. Although the shapes of the Loma Prieta perturbation at XHR and CWC (Figure 14) approximate the shapes of the classic creep event, the shapes of the perturbation at the remaining 6 sites is far from classic. Wesson (1988) has simulated composite events with somewhat similar shapes to those seen at XSJ and XMR in a model using multiple interacting slip patches each obeying a power-law rheology.

We note that the power law rheology as written, if applied to the fault at all depths, does not take into account the possibility of a sign change in τ at some depths that might temporarily reverse the creep direction. A better version might be written:

$$dU/dt = C\tau|\tau|^{n-1}$$

For small changes in stress, the power-law yields:

$$\frac{\Delta V}{V} = n\left(\frac{\Delta\tau}{\tau}\right)$$

where ΔV is the change in creeprate and $\Delta\tau$ is the change in driving stress, which motivated our use of the fractional creep rate change in the previous section. Comparison with equation (2) yields the result that

$$\frac{n}{\tau} \approx 8 \text{ bars}^{-1}$$

Again noting the inadequacies of equation (2), we can nonetheless infer a value for the "average" ambient stress on the fault plane under the creepmeters by substituting likely values for n. Crough and Burford (1977) report values of n between 1.0 and 2.5 with an average of 1.6 inferred from typical creep events. For such values, τ would lie between 0.1-0.3 bars which seems quite small, but which may represent average stress levels at the shallow depths most likely to be reflected in the first year of creeprate change.

Sharp and Saxton (1989) proposed an empirical law to describe the time-evolution of afterslip observed on the Superstition Hills fault after two earthquakes in November 1987:

$$U(t) = U_f \left(\frac{Bt}{1 + Bt} \right)^c$$

where U(t) is displacement at time t after the earthquake, and U_f, B, and c are constants. (L. Wennerberg (oral commun., 1993) has proposed a refined and better-fitting version of this empirical law.) Boatwright and others (1989) discuss an inversion method to infer the three parameters in the law from field data.

Scholz (1990) and Marone and others (1991) assumed a relation based on constitutive laws developed by Dieterich (1979, 1981), Ruina (1983), and Rice and Gu (1983) to explore the nature of afterslip curves. Their starting constitutive relation is:

$$\tau_{SS} = \tau_* + (A - B) \ln(V/V_*)$$

where T_{SS} is steady state frictional strength, V is sliding speed, $A - B$ is the friction rate parameter, and τ_* is the strength for steady state sliding at speed V_*. The afterslip displacement $U_p(t)$ at time t after the earthquake, is given by

$$U_p(t) = \frac{A - B}{k} \ln \left[\left(\frac{k V_{CS}^S}{A - B} \right) t + 1 \right] + V_o t$$

where k is the thickness averaged stiffness for the velocity strengthening region, V_{CS}^S is the thickness-averaged coseismic slip velocity within the velocity strengthening region, and V_o is the long term slip rate.

There is a difficulty in applying the constitutive relation when V becomes zero or negative. A more general formulation of the constitutive relation suggested by Dieterich (e.g., 1992) can

allow for these possibilities.

At depths of several kilometers, we would expect that the imposed shear stress changes under our creepmeter sites (typically tenths of bars or less) are small compared with the usual shear stress levels driving these faults. If so, then a linearized form of the above laws relating creeprate changes and stress changes may be appropriate, and the data provided by the creepmeters may not be adequate to distinguish among the various laws or, in fact, to distinguish them from a linear viscous response. The fact that the three sites that were close to regions where the fault surface had LL shear stress applied actually went LL for varying periods after Loma Prieta suggests that the usual shear stress levels in the upper meters or kilometers are normally quite small, and that the rheological laws governing this depth range on the fault can probably not be linearized. The behavior of the Middle Mountain creepmeter near Parkfield after the Coalinga earthquake (e.g., Mavko and others, 1985; Simpson and others, 1988) provides another example of such behavior.

Clearly, more work needs to be done to propose and test creeprate laws with the appropriate depth-dependent behaviors, in order to explain the perturbations at these creepmeters. One benefit of such a law will be the ability to calculate synthetic creep records at various sites based on the influences of nearby earthquakes. Once such a law is calibrated, it can also be used to infer the existence of stressing not obviously associated with seismicity, but perhaps caused by the passage of aseismic tectonic waves. Gwyther and others (1992) describe a post-Loma Prieta shear strain anomaly near San Juan Bautista recorded on a tensor strainmeter that could perhaps be used in conjunction with creep data to constrain a fault rheology.

If indeed the creep rates are responding to static stress changes caused by earthquakes, including earthquakes on other faults, this raises the question as to whether the effect is shallow or extends to depth. The creepmeters, if they are sitting over low-friction shallow cracks, could just be acting as sensitive strainmeters. The observation that microseismicity rates on Bay Area faults also responded to static stress changes after the Loma Prieta earthquake (Simpson and Reasenberg, 1992), suggests that some part of the observed changes in surface creep rates reflect changes in slip rate at seismogenic depths.

We have not attempted to fit any of these laws to the Loma Prieta perturbations displayed in Figure 14, partly because these perturbations are not very cleanly defined, and partly because we believe that the perturbations represent a composite response to sometimes complex stress distributions. We will instead attempt to use some simple dislocation models to put bounds on the total amount of perturbed slip that might occur at the various sites, and to estimate the depths that slip might be coming from as a function of time.

MODELS EXPLORING DEPTH-ORIGIN OF LOMA PRIETA AFTERSLIP

Although it is difficult to infer fault-zone rheology from the available "afterslip" observations, it is possible to estimate the depth to which the earthquake-induced anomalous slip extends. It might be the case, for example, that the afterslip recorded at the creepmeters was a superficial phenomenon, confined to the upper kilometer or two of the crust.

To bound the possible depth to which anomalous slip might extend, we used Okada's (1990) dislocation subroutines and the Loma Prieta slip distribution of Marshall and others (1990) to make a model of the San Andreas and Calaveras faults (Figure 15). Stress changes were calculated at the centers of 2 km x 2 km square dislocation patches extending down to 20 km. We permitted the dislocation squares between the Earth's surface and some chosen depth to slip freely in response to the earthquake-induced static stress changes, so that the stress at their centers was canceled. All squares below the chosen depth were not allowed to slip. No squares farther than 9 km north of creepmeter XSJ were allowed to slip in response to the stress changes. We assumed that the total slip in response to the stress changes would occur instantaneously, although, in fact, the slip must occur in viscous fashion over the space of several years.

The model contains an interruption in the Calaveras fault between HLC and HLD. This discontinuity, although small, will reduce the total slip estimated for nearby sites because of the fault connectivity effect of Bilham and Bodin (1992). (Sites on model faults that are distant from fault ends can slip farther than points close to ends of discontinuous segments.)

The results (Table 7, Figure 16) show, for example, that at CWC, 5 mm of anomalous surface slip at a maximum will occur if only the upper 2 km of the fault are able to respond to the stress changes. Figure 14 shows that slip at CWC had exceeded the amount expected at the pre-earthquake creep rate by this amount within several months of the earthquake, even if the coseismic step is not included. Compared to the creep rate in the year before the earthquake, at the beginning of 1993, anomalous excess slip of 30-35 mm had occurred at CWC (Figure 14), requiring anomalous slip to have occurred to depths in excess of 10 km in our model.

Figure 16 suggests that the total anomalous slip at the surface would not get much larger if even deeper levels were allowed to slip. We anticipate that the results obtained from a model where slip could extend to 50 km or 100 km would not be greatly different from the results observed at 20 km. As of July 1, 1992, observed anomalous slip advances and deficits were estimated to range from -25 to +45 mm for the 8 creepmeters on the San Andreas and Calaveras faults (Table 7). These observations fall within the calculated extremes of -28 to +60 mm in the 20-km column of Table 7. Because the anomalous slip is continuing, further comparisons will be needed.

The three-dimensional distribution of earthquake-induced shear stress in our model (Figure 15) suggests that efforts to infer fault-zone rheology from afterslip behavior recorded at the Earth's surface need to take into account the geometry of the stress field both laterally and with depth on the fault surface. For example, using the slip distribution of Marshall and others (1990), the

stresses imposed by the earthquake close to HLC and HLD are RL in the upper 6 km and LL from 6 to at least 20 km (Figure 15). The expected signal at these sites would initially be an increase in creep rate as the upper levels of the fault move faster in response to the added RL shear, followed by a slowing creep rate as the LL shear imposed at greater depths and to the north retards creep in these regions -- which eventually propagates to the creepmeter sites. One can see suggestions of such behavior in Figure 14 at sites HLC and HLD, although the "noise" level in these records is large enough to cast some doubt on this interpretation.

RETARDATION AND ANOMALOUS BEHAVIOR BEFORE THE EARTHQUAKE?

A number of possible precursors to the Loma Prieta earthquake have been suggested. For example Fraser-Smith and others (1990) reported anomalous electromagnetic radiations in the the days and hours before the earthquake. Gladwin and others (1991) described a strain anomaly near creepmeter XSJ that began mid-way through 1988. Galehouse (19--) suggested that some alinement arrays along the Hayward fault might have slowed down in the months before Loma Prieta, and Reasenberg and Simpson (19--) reported a possible slowdown in Hayward fault seismicity beginning in 1988.

We have listed four possible creep retardations (Table 2, Figure 4) that might have foreshadowed the Loma Prieta earthquake. We examined the retardation at CWC in detail because the behavior of CWC had been so consistent from about 1975 to 1987 that the retardation appears more convincing than do some of the others. We cannot rule out the possibility that drought conditions caused the slowdown at this site, but in the following we assume a tectonic origin and see where that leads.

An important observation is that in spite of possible retardations identified at XHR and XSJ (4 and 15 km northwest of CWC, respectively), the anomaly at CWC does not correspond very well in duration or character with the behaviors of neighboring creepmeters (Figures 2,3,4), suggesting that whatever is happening at CWC is mostly local in scope.

The Tres Pinos earthquake of 26 January 1986 ought to have increased the static shear stress at CWC by about 1/3 as much as the Loma Prieta event (Table 4), and our model suggests that these stress changes at CWC should have increased the creep rate just as the Loma Prieta earthquake did, rather than retard it. (A small increase in rate is apparent immediately after the Tres Pinos earthquake, but it was soon followed by the more obvious decrease.)

Another clue is offered in the detailed behavior of CWC during part of the retardation period (Figure 18). Although discrete RL events continued at about the same rate and size as before, a trend change in background movement beginning soon after a M3 earthquake on 871102 carries the instrument in a LL sense between the RL events. Histograms of creep step sizes for part of this period and for a more normal period are shown in Figure 19. Left-lateral movement between

RL events at CWC also took place between 1978 and 1981, but such behavior has not been the norm.

Bilham and Behr (1992) proposed a two-layer model for creep observed on the Superstition Hills fault. They described episodic creep events superimposed on a more constant background slip rate, and they proposed that the episodic slip is coming from deeper layers on the fault, while the background slip represents steady sliding in a near-surface layer. One plausible explanation for the CWC retardation would be to have the RL events produced by slip propagating to the surface from some region on the San Andreas fault under or adjacent to CWC. The LL slip between RL events would be produced by stress transferred to the San Andreas fault under CWC by slip on some other fault. The most obvious source is the Tres Pinos earthquake, which was followed by a diffuse set of aftershocks (Figure 20) suggesting regional stress changes in the complex region between the San Andreas and Calaveras faults (Burford and Savage, 1973). Afterslip on the Tres Pinos fault plane itself does not produce LL stresses near CWC with our model geometry. But if the Tres Pinos earthquake triggers RL slip on parts of the sub-parallel Calaveras/Paicines fault, the resultant stresses at CWC could be LL. Figure 21 (top) shows regions on nearby vertical faults where RL slip would produce LL stress at CWC.

A second scenario would be to have the Tres Pinos earthquake induce slip on some other structure even closer to CWC that could again induce LL stress changes on the San Andreas fault in the near surface under CWC. Small earthquakes define several such structures just to the north and east of CWC (Figure 20). Activation of a small structure close to CWC could explain why the effect is not seen with the same character on other nearby creepmeters. The next creepmeter 4 km to the north (XHR) might in fact see stresses of opposite polarity depending on the geometry and location of the slipping region. Future models will be constructed to test the magnitudes of slip needed on various nearby faults to produce the observed rates of LL stepping.

A third scenario would have regional, mostly aseismic slip on a sub-horizontal detachment structure following the Tres Pinos earthquake. Again, slip in the proper regions of such a structure could probably induce LL stress at CWC.

In all of these scenarios we suggest that the Tres Pinos earthquake caused or accompanied regional stress changes in the triangular wedge between the San Andreas and Calaveras faults, that could have been recorded at CWC as LL drift. Thus CWC retardation might have reflected large-scale stress changes that could also have triggered the Loma Prieta earthquake.

Perhaps it is significant that the region south of San Juan Bautista in which most creep retardations have been described (Burford, 1988) contains sub-parallel fault strands (San Andreas and Paicines/Calaveras). If RL slip were to alternate on these strands, then creepmeters on the moving strand would speed up, while those on the other would slow down. Perhaps when the slowed strand begins to move again the fault might have become more brittle because it has had a chance to heal, so that if sufficient stress has accumulated to produce an earthquake, then one would be more likely to occur at the end of a retardation period than at other times.

Burford (1988) suggested fault interactions of this sort as a possible explanation for the observed retardations. He also offers other explanations for the phenomenon, including growth of asperities, strain hardening, stress-waves, and fluctuation in driving stress. There appears to be some hope of evaluating these possibilities using simple dislocation models to explore plausible sources of imposed stresses.

CONCLUSIONS

Four mechanisms have been proposed to explain triggered slip (Allen and others, 1972; Fuis, 1982; Williams and others, 1988; McGill and others, 1989): (1) static stress changes produced by the earthquake rupture, (2) dynamic stresses from the passage of seismic waves, (3) creep migrating from the earthquake source region, and (4) a regional strain event that produces both aseismic slip on some faults as well as earthquakes on others.

The Loma Prieta earthquake produced coseismic steps on many of the central California creepmeters. We think that these steps were caused by shaking of the sites and the instruments, because they do not seem to correlate very well in either size or direction with calculated static stress changes, favoring explanation (2) above.

The Loma Prieta earthquake produced significant changes in average creep rate at a number of sites on the San Andreas, Calaveras, and Hayward faults (Galehouse, 19--). These changes are generally consistent in magnitude and sign with the static shear stress changes, and statistically significant correlations exist with three different models of the Loma Prieta rupture, although the quality of the correlations vary to some degree from model to model. The change in horizontal shear stress appears to be the significant variable. Changes in calculated normal stress do not seem to correlate at significant confidence levels, which suggests that coefficents of apparent friction are low for creep on these faults. A comparison of correlation coefficients for various assumed values of apparent coefficient of friction finds the best correlation for low values (0.0-0.3). These observations seem consistent with explanation (1) above. Explanation (3) might explain rate changes for creepmeters on the San Andreas fault, but hardly seems to explain the rate changes on the Calaveras or Hayward faults.

A 3-dimensional boundary element model was used to examine the depths that were being sampled by surface slip. This model can only put approximate limits on the depths that slip is "coming from", but suggests at CWC, for example, that by 1 year after the earthquake at the latest, slip from 10 km depth was being sampled at the surface. Total expected anomalous slip at the creep sites can also be estimated from this 3-dimensional model. The estimates range in value from -6 mm to 60 mm, which are in fair agreement with observed slip advances and deficits observed at the sites.

Rainfall-induced and seasonal variations in creepmeter behavior are considerable and raise the possibility that some rate variations that might be interpreted as precursors to earthquakes are

weather related. Because the drought conditions starting in 1987 were especially severe, creep retardations observed at four sites are suspect to some degree. We attempted to use creep behavior during the earlier drought years of 1976-1977 to calibrate the more recent drought, but found no strong link between climate and slip fluctuations.

Burford (1988) has proposed that creep retardations can occur at creep sites before local earthquakes, and has tabulated 25 instances of possible retardations on the San Andreas and Calaveras faults between 1957 and 1983. Assuming that a possible retardation at CWC that began in 1986-1987 and ended with the Loma Prieta earthquake might be of tectonic origin, we considered some possible tectonic causes of this retardation. The instrument continued to record large RL events during this interval but small LL slip events in the intervals between the large RL events slowed the total creep rate. This behavior is similar to that described by Bilham and Behr (1992), who ascribe the large creep steps and the background creep at creepmeter sites on the Superstition Hills fault to different sources. If such an explanation holds here, it would seem likely that the large RL steps that represent fairly normal behavior at CWC, come from slip on nearby parts of the San Andreas fault. We propose 3 scenarios for the origin of the LL drift: slip triggered on the Calaveras/Paicines fault, slip on a nearby structure to CWC revealed in the seismicity, or slip on a regional subhorizontal detachment. In all 3 scenarios, this movement would be triggered by regional tectonic adjustments following the 26 January 1986 Tres Pinos earthquake in the complex triangle (Burford and Savage, 1973) between the San Andreas and Calaveras faults. If this is correct, then the retardation at CWC could be regarded as a precursor to the Loma Prieta earthquake, if these same adjustments ultimately brought that earthquake closer to fruition. This scenario would also seem to give some credence to explanation (4) above as a viable mechanism.

The ability of the creepmeters to respond to Loma Prieta stress changes in predictable ways suggests to us that other regional stress-change information is contained in the creepmeter signals. It becomes increasingly important to understand the effects of weather and seasons on the instruments so that the true signals of tectonic origin can be extracted and interpreted.

ACKNOWLEDGEMENTS

This paper was greatly enchanced by discussion with Paul Reasenberg, Evelyn Roeloffs, John Langbein, Roger Bilham, Bob Burford, and Jeff Behr. We are also grateful to Rich Liechti, whose expertise in creepmeter maintenance ensures a foundation for this and other studies, and to Jon Galehouse and his students at San Francisco State University for reading the creepmeters manually during their surveying expeditions.

APPENDIX A: SITE NOTES

The following section provides further detail on conditions influencing the data from different creepmeters. These aspects are typically site-specific, and modulate the way we interpret the long-term record. As such they form the basis of several assumptions in this paper.

XHR: Combined datasets

The record for XHR used in the study is a composite of data from XHR1 and XHR2. Zero was lost on creepmeter XHR1 when it was destroyed in 1984 (Schulz 1989). To estimate a projected starting point for XHR2 data we calculated the amount of movement in a 245 day window, which is the duration of the gap between instruments, sliding the window every 10 days. The greatest change in a window with continuous data was 9.4 mm for the period ending 811102. We chose instead a correction value of 5.4 mm which occurred most often in the series of windows. Comparison with creep data from Cienega Winery, 3 km southeast of the site supports this as a reasonable adjustment for the level of activity at the time.

CWC: Instrument characteristics and rainfall

At the Winery, creepmeters actually measure offset of adjacent concrete floor slabs separated by the fault trace. Individual rainstorms produce only nominal changes in creep at this site. It is possible that a sustained drought might be expressed as a decrease in the background slip pattern such that episodic events, an indication of slip at depth, would be of normal amplitudes while inter-event slip could be more sensitive to changing conditions in the shallow soil. De-coupling between the instrument and the fault at this site makes the association between drought and slip deficit tentative at best. In fact, we could argue that the retardation seen at the Winery from 1987 to 1989 is caused by the same phenomenon that produced the slip deficit at XHR from late 1988 to September 1989. Perhaps both sites were responding to drought. Alternatively these instruments may have been sensing a local perturbation in fault activity that was over-ridden by the Loma Prieta earthquake.

Another instrument at the Winery, CWN, is not included in this study. At this creepmeter, located about 30 meters northwest of CWC, an obstruction gradually developed inside the instrument enclosure which inhibited the amount of movement recorded. Approximate onset of this condition is difficult to determine, and the slip released when the problem was corrected in February 1990 was insufficient to resolve the discrepancy between what was recorded on CWN and what was observed on CWC. Prior to 1987 the 2 instruments tracked each other very well, both in rate of slip and in creep event characteristics: onset, duration, and amplitude.

XMR: Rainfall and seismicity

We should again address the possibility that drought might be related to the creep retardation at Melendy Ranch since August 1988. In the long-term record the drought from 1975 to 1978 corresponds to a slip deficit at XMR. Burford (1988) asserts that this deficit was terminated by a M4.0 quake near the site in December 1977. Though the deficit is more firmly linked to seismicity, the drought also ended about this time making it difficult to isolate the effects. Another slip deficit in late 1982 to mid-1984 occurred when seasonal rainfall was normal, presenting one case where the seismic association is more obvious.

For the first 2.5 years of the current drought, creep at XMR was slightly accelerated after a M4.6 quake on January 14, 1986 terminated the retardation phase from late 1984 to the end of 1985 (Burford, 1988). It is unknown to what extent the slip slowdown which began in August 1988 is related to drought, or is a reflection of changes in local seismicity patterns. Creep rates at XMR

increased in mid-1991 and for the past 1.5 yeas have hovered close to the long-term average rate of 18 mm/year, as opposed to a rate of 13 mm/year following the Loma Prieta earthquake for the same duration. It is possible that the site is responding to the return of normal rainfall. Perhaps the most decisive clue will be the occurrence of the next M4-5 earthquake near this instrument. Until then the interpretive waters will continue to be muddied by the question of which variable is more dominant in the data: seismicity or rainfall.

XSH: Site modifications and rainfall

In Spring 1986 a new creepmeter was installed at Shore Road, slightly south of the original site and spanning an additional 5 meters of fault zone (Schulz 1989). The anchor pier of the new instrument is now within a few meters of an adjacent slough embankment. The stronger RL movement occurring during Winter and Spring may be related to increased movement of the anchor pier during wet weather. The fact that this pattern of activity was not seen at the site before 1987 adds credence to this account.

Aside from mechanical alterations it is worthwhile to explore what impact the drought might have in relation to the declining creep rate. Schulz and others (1983) describe a characteristic site response to rain, occurring as small oscillatory signals lasting a few days. This is evident throughout the data, both before and since 1986. A rain gauge was installed at this site in October 1992 to track creep with rainfall. Data from a single rainy season show a strong correlation between rainfall and movement on the creepmeter, which begins a few hours after onset of measurable precipitation. The previous drought from 1975 to 1978 was roughly coincident with the onset of creep retardation associated with the Coyote Lake earthquake. However, the slip deficit continued almost 2 years beyond the end of the drought, and rainfall-related movement is clearly evident during that period. During the pre-Morgan Hill creep retardation there was above average rainfall with no significant change in instrument response compared to the 1975-1979 deficit data. Thus it would appear that the current drought has less impact on the data than site modifications. Nevertheless a final verdict is premature until a more detailed study is conducted.

REFERENCES CITED

Allen, C.R., Wyss, M. Brune, J.N., Grantz, A., and Wallace, R.E., 1972, Displacements on the Imperial, Superstition Hills and the San Andreas faults triggered by the Borrego Mountain earthquake, in The Borrego Mountain earthquake of April 9, 1968: U.S. Geological Survey Professional Paper 787, p. 87-104.

Behr, J., Bilham, R., Bodin, P., Breckenridge, K., and Sylvester, A.G, 19--, Increased surface creep rates on the San Andreas fault southeast of the Loma Prieta mainshock, in, The Loma Prieta, California, earthquake of October 17, 1989: U.S. Geological Survey Professional Paper (in preparation).

Behr, J., Bilham, R., Bodin, P., Burford, R.O., and Burgmann, R., 1990, Aseismic slip on the San Andreas fault south of Loma Prieta: Geophysical Research Letters, v. 17, p. 1445-1448.

Beroza, G.C., 1991, Near-source modeling of the Loma Prieta earthquake: Evidence for heterogeneous slip and implications for earthquake hazard: Bulletin of the Seismological Society of America, v. 81, p. 1603-1621.

Bilham, R., 1989, Surface slip subsequent to the 24 November 1987 Superstition Hills, California, earthquake monitored by digital creepmeters: Bulletin of the Seismological Society of America, v. 79, p. 424-450.

Bilham, Roger, and Behr, Jeffrey, 1992, A two-layer model for aseismic slip on the Superstition Hills fault, California: Bulletin of the Seismological Society of America, v. 82, p. 1223-1235.

Bilham, Roger, and Bodin, Paul, 1992, Fault zone connectivity: Slip rates on faults in the San Francisco Bay Area, California: Science, v. 258, p. 281-284.

Boatwright, John, Budding, K.E., and Sharp, R.V., 1989, Inverting measurements of surface slip on the Superstition Hills fault: Bulletin of the Seismological Society of America, v. 79, p. 411-423.

Breckenridge, K.S., and Burford, R.O., 1990, Changes in fault slip near San Juan Bautista, California before the October 17, 1989 Loma Prieta earthquake - A possible precursor?: Eos, Transactions, American Geophysical Union, v. 71, p. 1461.

Burford, R.O., 1972, Continued slip on the Coyote Creek fault after the Borrego Mountain earthquake, in The Borrego Mountain Earthquake of April 9, 1968: U.S. Geological Survey Professional Paper 787, p. 105-111.

Burford, R.O., 1988, Retardations in fault creep rates before local moderate earthquakes along the San Andreas fault system, central California: PAGEOPH, v. 126, p. 499-529.

Burford, R.O., Allen, SS., Lamson, R.J., and Goodreau, D.D., 1973, Accelerated fault creep along the central San Andreas fault after moderate earthquakes during 1971-1973: in Kovach, R.L., and Nur, Amos, eds., Proceedings of the Conference on Tectonic Problems of the San Andreas Fault System: Geological Sciences, Volume XIII, School of Earth Sciences, Stanford University, p. 275-285.

Burford, R.O., and Savage, J.C., 1972, Tectonic evolution of a crustal wedge caught within a transform fault system: Geological Society of America Abstracts with Programs, v. 4, p. 134.

Cohn, S.N., Allen, C.R., Gilman, R., and Goulty, N.R., 1982, Preearthquake and postearthquake creep on the Imperial fault and the Brawley fault zone, in The Imperial Valley, California, Earthquake of October 15, 1979: U.S. Geological Survey Professional Paper 1254, p. 161-167.

Crough, S.T., and Burford, R.O., 1977, Empirical law for fault-creep events: Tectonophysics, v. 42, p. 53-59.

Dieterich, J.H., 1979, Modeling of rock friction, 1. Experimental results and constitutive equations: Journal of Geophysical Research, v. 84, p. 2161-2168.

Dieterich, J.H., 1981, Constitutive properties of faults with simulated gouge, in Carter, N.L., Friedman, M., Logan, J.M., and Stearns, D.W., eds., Mechanical Behavior of Crustal Rocks: American Geophysical Union, Geophysical Monograph 24, p. 103-120.

Dieterich, J.H., 1992, Earthquake nucleation on faults with rate- and state-dependent strength: Tectonophysics, v. 211, p. 115-134.

Fagerson, S.H., Louie, J.N., Allen, C.R., Sieh, K.E., 1986, Measurements of triggered slip on the southern San Andreas fault associated with the North Palm Springs earthquake: Eos, Transactions, American Geophysical Union, v. 67, p. 1090.

Fraser-Smith, A.C., Bernardi, A., McGill, P.R., Ladd, M.E., Helliwell, R.A., and Villard, O.G., Jr., 1990, Low-frequency magnetic field measurements near the epicenter of the Ms 7.1 Loma Prieta earthquake: Geophysical Research Letters, v. 17, p. 1465-1468.

Fuis, G.S., 1982, Displacement on the Superstition Hills fault triggered by the earthquake, in the Imperial Valley, California, Earthquake of October 15, 1979: U.S. Geological Survey Professional Paper 1254, p. 145-154.

Galehouse, J.S., 1990, Effect of the Loma Prieta earthquake on surface slip along the Calaveras fault in the Hollister area: Geophysical Research Letters, v. 17, p. 1219-1222.

Galehouse, J.S., 1992, Creep rates and creep characteristics on certain North and East Bay faults: 1979-1992: Programs and Abstracts, Second Conference on Earthquake Hazards in the Eastern San Francisco Bay Area, March 25-29, 1992, California State University, Hayward, p. 24.

Galehouse, J.S., 19--, Effect of the Loma Prieta earthquake on fault creep rates in the San Francisco Bay region, in, The Loma Prieta, California, earthquake of October 17, 1989: U.S. Geological Survey Professional Paper (in preparation).

Gladwin, M.T., Gwyther, R.L., Higbie, J.W., and Hart, R.G., 1991, A medium term precursor to the Loma Prieta Earthquake?: Geophysical Research Letters, v. 18, p. 1377-1380.

Goulty, Neil R., and Gilman, Ralph, 1978, Repeated creep events on the San Andreas Fault near Parkfield, California, recorded by a strainmeter array: Journal of Geophysical Research, v. 83, no. B11, p. 5414-5419.

Gwyther, R. L., Gladwin, M. T., and Hart, R. G., 1992, A shear strain anomaly following the Loma Prieta earthquake: Letters to Nature, v. 356, p. 142-144.

Hartzell, S.H., and Heaton, T.H., 1986, Rupture history of the 1984 Morgan Hill, California, earthquake from the inversion of strong motion records: Bulletin of the Seismological Society of America, v. 76, 649-674.

Hudnut, K.W., and Clark, M.M., 1989, New slip along parts of the Coyote Creek fault rupture, California: Bulletin of the Seismological Society of America, v. 79, p. 451-465.

Johnston, M.J.S., Linde, A.T., Gladwin, M.T., and Borcherdt, R.D., 1987, Fault failure with moderate earthquakes: Tectonophysics, v. 144, p. 189-206.

Johnston, M.J.S., Linde, A.T., and Gladwin, M.T., 1990, Near-field high resolution strain measurements prior to the October 18, 1989, Loma Prieta Ms 7.1 earthquake: Geophysical Research Letters, v. 17, p. 1777-1780.

King, C.Y., Nason, R.D., and Burford, R.O., 1977, Coseismic steps recorded on creep meters along the San Andreas fault: Journal of Geophysical Research, v. 82, p. 1655-1662.

Langbein, John, Quilty, Eddie, and Breckenridge, Katherine, 1993, Sensitivity of crustal deformation instruments to changes in secular rate: Geophysical Research Letters, v. 20, no. 2, p. 85-88.

Lisowski, M., Prescott, W.H., Savage, J.C., and Johnston, M.J., 1990, Geodetic estimate of coseismic slip during the 1989 Loma Prieta, California, Earthquake: Geophysical Research Letters, v. 17, p. 1437-1440.

Marone, C.J., Scholz, C.H., and Bilham, R., 1991, On the mechanics of earthquake afterslip: Journal of Geophysical Research, v. 96, p. 8441-8452.

Marshall, G.A., Stein, R.S., and Thatcher, Wayne, 1991, Faulting geometry and slip from coseismic elevation changes: the 18 October 1989, Loma Prieta, California, earthquake: Bulletin of the Seismological Society of America, v. 81, p. 1660-1693.

Mavko, G. M., 1982, Fault interaction near Hollister, California: Journal of Geophysical Research, v. 87, p. 7807-7816.

Mavko, G.M., Schulz, S., and Brown, B.D., 1985, Effects of the 1983 Coalinga, California, earthquake on creep along the San Andreas fault: Bulletin of the Seismological Society of America, v. 75, p. 475-489.

McClellan, P.H., and Hay, E.A., 1990, Triggered slip on the Calaveras fault during the magnitude 7.1 Loma Prieta, California, earthquake: Geophysical Research Letters, v. 17, p. 1227-1230.

McGill, S.F., Allen, C.R., Hudnut, K.W., Johnson, D.C., Miller, W.F., and Sieh, K.E., 1989, Slip on the Superstition Hills fault and on nearby faults associated with the 24 November 1987 Elmore Ranch and Superstition Hills earthquakes, southern California: Bulletin of the Seismological Society of America, v. 79, p. 362-375.

Nason, R.D., 1973, Fault creep and earthquakes on the San Andreas fault: in Kovach, R.L., and Nur, Amos, eds., Proceedings of the Conference on Tectonic Problems of the San Andreas

Fault System: Geological Sciences, Volume XIII, School of Earth Sciences, Stanford University, p. 275-285.

Nason, R.D., and, Weertman, Johannes, 1973, A dislocation theory analysis of fault creep events: Journal of Geophysical Research, v. 78, p. 7745-7751.

Okada, 1992, Internal deformation due to shear and tensile faults in a half-space: Bulletin of the Seismological Society of America, v. 82, p. 1018-1040.

Oppenheimer, D.H., Bakun, W.H., and Lindh, A.G., 1990, Slip partitioning of the Calaveras fault, California, and prospects for future earthquakes: Journal of Geophysical Research, v. 95, p. 8483-8498.

Oppenheimer, D.H., Reasenberg, P.A., and Simpson, R.W., 1988, Fault plane solutions fro the 1984 Morgan Hill, California, earthquake sequence: Evidence for the state of stress on the Calaveras fault: Journal of Geophysical Research, v. 93, p. 9007-9026.

Reasenberg, P.A., and Simpson, R.W., 1992, Response of regional seismicity to the static stress change produced by the Loma Prieta earthquake: Science, v. 255, p. 1687-1690.

Reasenberg, P.A., and Simpson, R.W., 19--, Response of regional seismicity to earthquake-induced the static stress changes, in Reasenberg, P.A., ed., The Loma Prieta, California, earthquake of October 17, 1989--postseismic effects, aftershocks, and other phenomena: U.S. Geological Survey Professional Paper 1550-D (in preparation).

Rice, J.R., and Gu, Ji-cheng, 1983, Earthquake aftereffects and triggered seismic phenomena: Pageoph, v. 121, p. 185-219.

Ruina, A. L., 1983, Slip instability and state variable friction laws: Journal of Geophysical Research, v. 88, p. 10359-10370.

Sachs, Lothar, 1982, Applied statistics - A handbook of techniques: New York, Springer-Verlag, 706 p.

Savage, J. C., and Burford, R. O., 1973, Strain accumulation in California: Bulletin of the Seismological Society of America, v. 60, p. 6469-6479.

Scholz, C. H., Wyss, M., and Smith, S. W., 1969, Seismic and aseismic slip on the San Andreas fault: Journal of Geophysical Research, v. 74, p. 2049-2069.

Scholz, C.H., 1990, The mechanics of earthquakes and faulting: Cambridge, U.K., Cambridge University Press, 439 p.

Schulz, S.S., 1984, Triggered creep near Hollister after the April 24, 1984, Morgan Hill, California, earthquake, in, Bennett, J.H., and Sherburne, R.W., eds., The 1984 Morgan Hill, California Earthquake: California Division of Mines and Geology Special Publication 68, p. 175-182.

Schulz, S.S., 1989, Catalog of creep measurements in California from 1966 to 1988: U.S. Geological Survey Open-File Report 78-203, 193 p.

Schulz, S.S., Burford, R.O., and Mavko, B., 1983, Influence of seismicity and rainfall on episodic creep on the San Andreas fault system in central California: Journal of Geophysical Research, v. 88, p. 7475-7484.

Schulz, S.S., Mavko, G.M., Brown, B.D., 1987, Response of creepmeters on the San Andreas fault near Parkfield to the May 2, 1983, Coalinga earthquake: U.S. Geological Survey Professional Paper 1487, p. 409-417.

Schulz, S.S., Mavko, G.M., Burford, R.O., and Stuart, W.D., 1982, Long-term fault creep observations in central California: Journal of Geophysical Research, v. 87, p. 6977-6982.

Sharp, R.V., 1989, Pre-earthquake displacement and triggered displacement on the Imperial fault associated with the Superstition Hills earthquake of 24 November 1987: Bulletin of the Seismological Society of America, v. 79, p. 466-479.

Sharp, R.V., Rymer, M.J., and Lienkaemper, J.J., 1986a, Surface displacements on the Imperial and Superstition Hills faults triggered by the Westmorland, California, earthquake of 26 April 1981: Bulletin of the Seismological Society of America, v. 76, p. 949-965.

Sharp, R.V., Rymer, M.J., and Morton, D.M., 1986b, Trace-fractures on the Banning fault created in association with the 1986 North Palm Springs earthquake: Bulletin of the Seismological Society of America, v. 76, p. 1838-1843.

Sharp, R.V., and Saxton, J.L., 1989, Three-dimensional records of surface displacement on the Superstition Hills fault zone associated with the earthquakes of 24 November 1987: Bulletin of the Seismological Society of America, v. 79, p. 376-389.

Shimada, Seiichi, Sakata, Shoji, and Noguchi, Shin'ichi, 1987, Coseismic strain steps observed by three-component borehole strainmeters: Tectonophysics, v. 144, p. 207-214.

Sieh, K.E., 1982, Slip along the San Andreas fault associated with the earthquake, in the Imperial Valley, California, Earthquake of October 15, 1979: U.S. Geological Survey Professional Paper 1254, p. 155-159.

Silverman, S., Mortensen, C., and Johnston, M., 1989, A Satellite-based digital data system for low-frequency geophysical data: Bulletin of the Seismological Society of America, v. 79, p. 189-198.

Simpson, R.W., and Reasenberg, P.A., 1994, Earthquake-induced static stress changes on central California faults, in Simpson, R.W., ed., The Loma Prieta, California, earthquake of October 17, 1989--tectonic processes and models: U.S. Geological Survey Professional Paper 1550-F.

Simpson, R.W., Schulz, S.S., Dietz, L.D., and Burford, R.O., 1988, The response of creeping parts of the San Andreas fault to earthquakes on nearby faults: Two examples: PAGEOPH, v. 126, p. 665-685.

Smith, S.W., and Wyss, Max, 1968, Displacement on the San Andreas fault subsequent to the 1966 Parkfield earthquake: Bulletin of the Seismological Society of America, v. 58, p. 1955-1973.

Spudich, Paul, Steck, L.K., Hellweg, Margaret, Fletcher, J.B., and Baker, L.M., 1993, Transient stresses at Parkfield, California, produced by the M7.4 Landers earthquake of June 28, 1992: Observations from the Upsar dense seismograph array: Journal of Geophysical Research, in press.

U.S. Department of Commerce, National Oceanic and Atmospheric Administration. Climatological Data, California. Ashville, NC: National Climatic Data Center, 1970-1992.

Wesson, R.L., 1987, Modelling aftershock migration and afterslip of the San Juan Bautista, California, earthquake of October 3, 1972: Tectonophysics, v. 144, p.215-229.

Wesson, R.L., 1988, Dynamics of fault creep: Journal of Geophysical Research, v. 93, p. 8929-8951.

Wesson, R.L., Jibson, R.W., Morton, D., Campbell, R.H., and Nicholson, C., 1986, Interpretation of surface cracks and other fault-line surface deformation associated with the North Palm Springs earthquake of July 8, 1986: Eos, Transactions, American Geophysical Union, v. 67, p. 1090.

Wesson, R.L., and Nicholson, Craig, 1988, Intermediate-term, pre-earthquake phenomena in California, 1975-1986, and preliminary forecast of seismicity for the next decade: Pageoph, v. 126, p. 407-446.

Williams, P., Fagerson, S., and Sieh, K., 1986, Triggered slip of the San Andreas fault after the July 8, 1986 North Palm Springs earthquake: Eos, Transactions, American Geophysical Union, v. 67, p. 1090.

Williams, P.L., McGill, S.F., Sieh, K.E., Allen, C.R., and Louie, J.N., 1988, Triggered slip along the San Andreas fault after the 8 July 1986 North Palm Springs earthquake: Bulletin of the Seismological Society of America, v. 78, p. 1112-1122.

TABLE CAPTIONS

TABLE 1. Summary table of all USGS creepmeters in operation at the time of the Loma Prieta earthquake. A * in first column indicates a site on the Southwest Fracture near Parkfield. A * in the coseismic change column indicates initial RL movement which was offset by subsequent LL movement within hours to days of the earthquake. Question marks in the coseismic change column indicate lack of data for determining coseismic movement. Negative values indicate left-lateral coseismic steps, positive are right-lateral.

TABLE 2. Possible creep retardations before the earthquake. The retarded rate and the background rate were determined by fitting least square lines to the intervals of interest. The background interval extends from the origin of the respective meter to 10/17/89.

TABLE 3. Average creep rates for 5 creepmeters on the San Andreas Fault and 3 creepmeters on the Calaveras fault. Average rate is determined by least square fitting of a line to data in either a 6-month window (a) or in a 1-year window (b); the windows are advanced by 3-month and half-year increments, respectively, over the period of interest, and the resulting rates are averaged. The first interval is a background period which ends more than 3 years before the earthquake so as to avoid possible precursory Loma Prieta effects. The second interval includes possible precursory Loma Prieta effects. The third interval is for 1 year after the earthquake. The fourth interval is for 2 years after the earthquake. Negative values indicate left-lateral rates, positive are right-lateral.

TABLE 4. Observed coseismic steps and 1-year average rates for 8 creepmeters and 6 earthquakes. The earthquakes in column 1 are ch = Chittenden, lp = Loma Prieta, tp = Tres Pinos, mh = Morgan Hill, cl = Coyote Lake, td = Thanksgiving Day. For coseismic steps in column 3, '-' indicates no step, and '?' indicates that the data were not available. 1-Year average rates were calculated by fitting a least-squares to the data in the one year interval and ignoring any coseismic offset. Fractional rate change in column 6 is calculated from columns 4 and 5 as (ratebefore-rateafter)/ratebefore. Stress changes in columns 7 and 8 were calculated from dislocation models described in TABLE 3 and in the text. Negative values indicate left-lateral changes or rates, positive are right-lateral.

TABLE 5. Values used in dislocation models of the six earthquakes. Negative horizontal-slip values indicate left-lateral, positive are right-lateral. Negative dip-slip value indicates reverse faulting. Earthquake information from Oppenheimer and others (1990).

TABLE 6. Statistical tests to determine significance of relation between changes in 1-year average creep rates and calculated changes in static stress.

TABLE 7. Total post-Loma Prieta anomalous slip at 8 creepmeters predicted for various depths to the bottom of the freely-slipping layer. Calculations based on a dislocation model using the Loma Prieta slip distribution of Marshall and others (1990). Negative values indicate left-lateral slip, positive are right-lateral. The values shown in the last 2 columns are observed anomalous slip as of July 1, 1992 relative to a 1-year average rate before Loma Prieta (Observed1, see FIGURE 14) and relative to a 3-year average rate before Loma Prieta (Observed3).

Table 1

Site	Fault	Origin (mo/yr)	Sample Rate	Distance from Loma Prieta (km)	Coseismic Change (mm)	Post-LP Rate Change(?)
XSJ	San Andreas	11/74	10 minute	39	5.2 *	Y
XHR	San Andreas	9/70	10 minute	50	4.3	Y
CWC	San Andreas	10/68	10 minute	54	6.8	Y
XFL	San Andreas	4/73	10 minute	68	-0.35	Y
XMR	San Andreas	6/69	10 minute	79	2.6	?
MRW	San Andreas	10/72	quarterly	80	?	Y
BIT	San Andreas	7/69	quarterly	107	?	N
XMP	San Andreas	6/69	quarterly	133	?	N
XSC	San Andreas	6/69	10 minute	155	0.2	N
XMM	San Andreas	9/79	10 minute	171	0.7	?
XMD	San Andreas	7/86	10 minute	174	1.8	N
XVA	San Andreas	4/87	10 minute	177	3.1	N
XRS*	San Andreas	5/87	10 minute	178	-0.01	N
XPK	San Andreas	9/79	10 minute	180	1.5	N
XTA	San Andreas	9/85	10 minute	182	0.14	N
WKR	San Andreas	9/76	10 minute	186	0.8	N
XHS*	San Andreas	6/87	10 minute	184	0.1	N
CRR	San Andreas	6/66	10 minute	190	0.03	N
XGH	San Andreas	6/69	10 minute	192	0.06	N
X46	San Andreas	8/86	10 minute	204	0.2	N
HWR	Hayward	4/68	quarterly	73	?	N
HWE	Hayward	4/68	quarterly	72	?	N
HWW	Hayward	4/68	quarterly	72	?	Y
HWP	Hayward	5/70	quarterly	71	?	?
XSH	Calaveras	6/71	10 minute	40	5.1 *	Y
HLC	Calaveras	4/70	quarterly	47	?	Y
HLD	Calaveras	4/70	quarterly	48	?	Y

Table 2 - Possible Creep Retardations Before the Earthquake

Site	From	To	Duration (months)	Rate (mm/yr)	Background Rate (mm/yr)
XSJ	August 1982	April 1990	92	3.8	6.4
XHR	September 1988	September 1989	12	6.1	7.5
CWC	August 1987	October 1989	26	6.9	10.1
XMR	August 1988	May 1991	36	12.3	18.0
XSH	May 1989	continuing	30	-0.3	11.8

Table 3 - Average creep rates for various intervals.

(A)

6-Month Average Creep Rates, in mm/yr

Interval Dates:	01/01/77-01/01/86	01/01/86-10/01/89	11/01/89-11/01/90	11/01/89-11/01/91
XSJ	6.1 ± 7.1 (35)	4.1 ± 5.8 (14)	15.1 ± 7.7 (3)	14.5 ± 6.0 (7)
XHR	7.7 ± 3.7 (25)	8.5 ± 4.0 (12)	22.0 ± 3.3 (3)	19.2 ± 4.4 (7)
CWC	10.3 ± 3.8 (30)	8.1 ± 3.9 (14)	18.4 ± 4.1 (3)	15.8 ± 5.1 (7)
XFL	6.3 ± 3.7 (28)	7.3 ± 3.1 (14)	15.0 ± 3.1 (3)	11.3 ± 4.2 (7)
XMR	17.4 ± 8.0 (34)	18.1 ± 9.3 (14)	12.1 ± 2.0 (3)	13.4 ± 5.3 (7)
XSH	13.1 ±15.9 (33)	9.5 ±15.2 (12)	0.1 ± 5.7 (3)	-1.6 ±10.5 (7)
HLC	12.0 ±12.1 (19)	--- (0)	-1.6 ± 5.3 (3)	0.6 ± 4.5 (6)
HLD	8.0 ± 3.1 (2)	--- (0)	-0.3 ± 1.9 (3)	-1.0 ± 1.5 (6)

The 6-month sampling interval advances in 3-month steps. First number is average creep rate in mm/yr; second number after ± is one standard deviation; value in parentheses is the number of 6 month intervals within the overall interval that were used to calculate average and standard deviation.

(B)

1-Year Average Creep Rates, in mm/yr

Interval Dates:	01/01/77-01/01/86	01/01/86-10/01/89	11/01/89-11/01/90	11/01/89-11/01/91
XSJ	6.0 ± 4.9 (17)	4.3 ± 3.4 (6)	15.0 ± -- (1)	14.3 ± 1.0 (3)
XHR	7.9 ± 2.4 (14)	8.5 ± 2.3 (6)	23.0 ± -- (1)	20.2 ± 4.2 (3)
CWC	10.4 ± 1.4 (17)	8.0 ± 1.6 (6)	18.2 ± -- (1)	15.1 ± 2.7 (3)
XFL	6.6 ± 2.1 (14)	7.6 ± 1.3 (6)	14.8 ± -- (1)	11.0 ± 3.3 (3)
XMR	17.0 ± 5.0 (17)	17.7 ± 7.7 (6)	12.8 ± -- (1)	13.6 ± 1.6 (3)
XSH	12.7 ±11.1 (17)	6.6 ± 9.4 (5)	0.1 ± -- (1)	-0.7 ± 4.1 (3)
HLC	10.2 ± 6.3 (15)	4.6 ± 4.1 (6)	-1.3 ± -- (1)	0.7 ± 1.8 (3)
HLD	1.9 ± 2.3 (14)	1.5 ± 1.8 (6)	0.3 ± -- (1)	-0.8 ± 1.0 (3)

The 1-year sampling interval advances in half-year steps. First number is average creep rate in mm/yr; second number after ± is one standard deviation; value in parentheses is the number of half-year intervals within the overall interval that were used to calculate average and standard deviation.

Table 4 - Creepmeter Response to Earthquakes

Earthquake	Creep-meter	Coseismic Step (mm)	1-Year Rate Before (mm/yr)	1-Year Rate After (mm/yr)	Fractional Rate Change	Shear Stress (bars)	Normal Stress (bars)
ch	XSH	-0.04	7.0	2.1	-0.70	-0.07	-0.17
ch	HLC	?	12.2	1.5	-0.88	-0.03	-0.01
ch	HLD	?	7.1	-1.1	-1.15	-0.02	0.00
ch	XSJ	-	8.3	13.6	0.64	0.09	-0.02
ch	XHR	5.40	27.6	22.7	-0.18	0.02	0.00
ch	CWC	3.80	27.3	13.5	-0.51	0.01	0.00
ch	XFL	0.15	8.6	9.0	0.05	0.00	0.00
ch	XMR	-	15.6	13.2	-0.15	0.00	0.00
lp	XSH	4.40	2.3	0.8	-0.65	-0.27	-0.69
lp	HLC	?	1.0	-1.3	-2.30	-0.19	-0.17
lp	HLD	?	1.5	0.3	-0.80	-0.15	-0.11
lp	XSJ	4.00	2.0	14.2	6.10	0.64	-0.19
lp	XHR	4.30	6.3	22.8	2.62	0.32	-0.12
lp	CWC	6.80	6.9	18.8	1.72	0.25	-0.10
lp	XFL	-0.35	7.5	14.9	0.99	0.12	-0.03
lp	XMR	2.60	8.7	12.5	0.44	0.08	-0.02
tp	XSH	-	21.8	10.8	-0.50	-0.02	0.00
tp	HLC	-	1.5	-0.7	-1.47	-0.07	-0.03
tp	HLD	?	6.9	1.5	-0.78	-0.06	-0.06
tp	XSJ	-0.05	3.7	3.9	0.05	-0.03	-0.02
tp	XHR	2.68	9.2	4.2	-0.54	0.05	-0.05
tp	CWC	1.54	9.3	8.8	-0.05	0.09	0.00
tp	XFL	-0.05	7.7	7.6	-0.01	0.01	-0.05
tp	XMR	0.35	13.4	22.4	0.67	0.02	-0.01
mh	XSH	13.00	5.0	21.0	3.20	0.18	0.01
mh	HLC	?	1.0	15.9	14.90	0.07	0.01
mh	HLD	?	1.0	1.3	0.30	0.06	0.00
mh	XSJ	-	5.8	1.0	-0.83	-0.10	0.06
mh	XHR	0.50	3.9	6.0	0.54	-0.02	0.00
mh	CWC	0.31	9.4	8.3	-0.12	-0.01	-0.01
mh	XFL	-	3.6	5.1	0.42	0.01	-0.01
mh	XMR	0.27	12.2	14.1	0.16	0.01	0.00
cl	XSH	8.90	2.4	11.6	3.83	0.31	-0.01
cl	HLC	?	1.7	11.2	5.59	0.08	0.00
cl	HLD	?	0.2	0.1	-0.50	0.06	0.00
cl	XSJ	-	3.6	5.2	0.44	-0.10	0.07
cl	XHR	-	3.0	7.8	1.60	-0.01	-0.01
cl	CWC	-	9.9	11.6	0.17	0.00	-0.01
cl	XFL	-	5.8	20.0	2.45	0.01	-0.01
cl	XMR	-	17.1	11.8	-0.31	0.01	0.00
td	XSH	?	18.2	23.8	0.31	-0.19	0.08
td	HLC	?	16.3	13.0	-0.20	-0.15	-0.04
td	HLD	?	1.1	3.4	2.09	-0.10	-0.01
td	XSJ	0.30?	9.0	12.0	0.33	-0.05	-0.13
td	XHR	?	9.0	7.8	-0.13	0.03	-0.01
td	CWC	-	8.8	9.5	0.08	0.01	0.00
td	XFL	-	9.9	8.0	-0.19	0.00	0.00
td	XMR	-	19.0	20.7	0.09	0.00	0.00

Table 5 - Parameters for Six Earthquake Models

date	name	M	no.	lon (deg)	lat (deg)	depth (km)	len. (km)	ht. (km)	strike (deg)	dip (deg)	horiz slip (m)	dip slip (m)
741128	Thanksgiving Day	5.1	1	121.46	36.92	4.5	1	1	33	90	-1.5	0
790806	Coyote Lake	5.9	1	121.53	37.10	6.0	13	8	335	90	0.2	0
840424	Morgan Hill §	6.2	324	121.61	37.22	-	27	12	328	90	0.24§	0
860126	Tres Pinos	5.3	1	121.28	36.80	7.5	1	1	353	83	3.0	0
891018	Loma Prieta †	7.0	1	121.91	37.06	11.2	37	13.3	136	70	1.66	-1.19
900418	Chittenden	5.4	1	121.64	36.94	4.8	1	1	312	90	4.2	0

M = local magnitude

no. = number of elements in dislocation model

depth = depth to center of model

len. = horizontal length of rectangular dislocation surface

ht. = down-dip dimension of rectangular dislocation surface

strike, dip = orientation of rectangular dislocation surface

horiz. slip = component of slip in horizontal direction

dip slip = component of slip in down-dip direction

§ Model based on Harzell and Heaton (1986) used by Oppenheimer and others (1988). Slip value is average.

† This is the Lisowski model described in Simpson and Reasenberg (19??)

Table 6 - Statistics for Relation of Creep Rates and Stress Changes

Earthquake Model(s)	Stress Component	Depth (km)	Two-Sided Chi-sq	Confidence (%)	Rho	N	Conf (%)	Slope0 (bar^{-1})	Slope (bar^{-1})	Intercept
L	horiz. shear	0	8.00	99	0.96	8	99	8.38	8.16±0.97	0.19±0.29
B	"	"	4.44	96	0.90	8	99	4.16	4.14±0.83	0.03±0.48
M	"	"	1.90	83	0.87	8	99	4.75	4.74±1.08	0.01±0.53
L	normal	0	NA	0	0.18	8	<50	-1.32	2.10±4.80	1.39±1.29
B	"	"	0.53	53	-0.71	8	95	-6.55	-7.04±2.88	1.19±0.70
M	"	"	4.44	96	-0.50	8	<80	-5.50	-4.77±3.35	0.53±0.92
L	horiz. shear	10	8.00	99	0.88	8	99	6.50	6.34±1.36	0.88±0.46
B	"	"	8.00	99	0.86	8	99	4.38	4.17±1.02	0.71±0.51
M	"	"	8.00	99	0.85	8	99	5.05	4.79±1.21	0.66±0.52
L	normal	10	NA	0	0.30	8	<50	-0.03	2.48±3.22	1.54±1.16
B	"	"	0.53	53	0.13	8	<50	0.28	0.78±2.50	1.14±1.06
M	"	"	1.90	83	0.08	8	<50	0.74	0.57±2.79	1.12±1.10
ALL	horiz. shear	0	3.88	95	0.48	48	99	9.35	8.81±2.36	0.60±0.34
ALL>0.05	"	"	6.58	98	0.48	25	98	9.39	8.38±3.23	1.06±0.64
ALL	normal	0	0.30	41	0.07	48	<50	-0.82	1.58±3.50	0.83±0.41
ALL>0.05	"	"	0.88	65	0.00	14	0	-0.88	0.02±3.16	0.35±0.68
ALL	horiz. shear	10	6.50	99	0.45	48	99	8.51	8.09±2.36	0.66±0.34
ALL>0.05	"	"	9.38	99	0.46	20	96	8.48	7.72±3.52	1.45±0.79
ALL	normal	10	0.23	36	0.08	48	<50	0.24	1.48±2.57	0.82±0.39
ALL>0.05	"	"	0.20	34	0.13	11	<50	0.28	1.06±2.64	0.52±0.84

Models: L=Lisowski, B=Beroza, M=Marshall, ALL=Lisowski plus 5 other earthquakes, ALL>0.05 = same as ALL except with stress changes less than 0.05 bar omitted.

Depth = depth at which static stress changes were calculated.

Two-sided Chi-sq = Confidence that the fractional creep rate and change in stress component are not independent based on the two-sided Chi sqaured test applied to the respective four-fold table (Sachs, 1982).

Rho = Correlation coefficient for fractional creep rates and static stress change values.

N = number of samples.

Conf = Confidence in best fit line.

Slope0 = Slope of best fit line forced to pass through the origin.

Slope, Intercept = Parameters for best fit line not forced to pass through the origin.

Table 7. - Post-Loma Prieta Anomalous Slip, in mm

depth->	2km	4km	6km	10km	20km	Observed(1)	Observed(3)
XSJ	18.8	30.8	39.1	49.4	60.3	30	25
XHR	6.2	12.1	17.7	27.5	41.8	45	33
CWC	4.7	9.0	13.5	21.9	35.4	30	33
XFL	1.9	3.5	5.4	9.7	19.4	7	7
XMR	1.2	2.1	3.1	5.6	12.2	20	-10
XSH	-7.0	-11.4	-14.6	-19.7	-28.6	-7	-25
HLC	0.1	-1.2	-2.8	-5.9	-10.5	5	-15
HLD	0.2	-0.7	-1.6	-3.3	-5.7	-5	-5

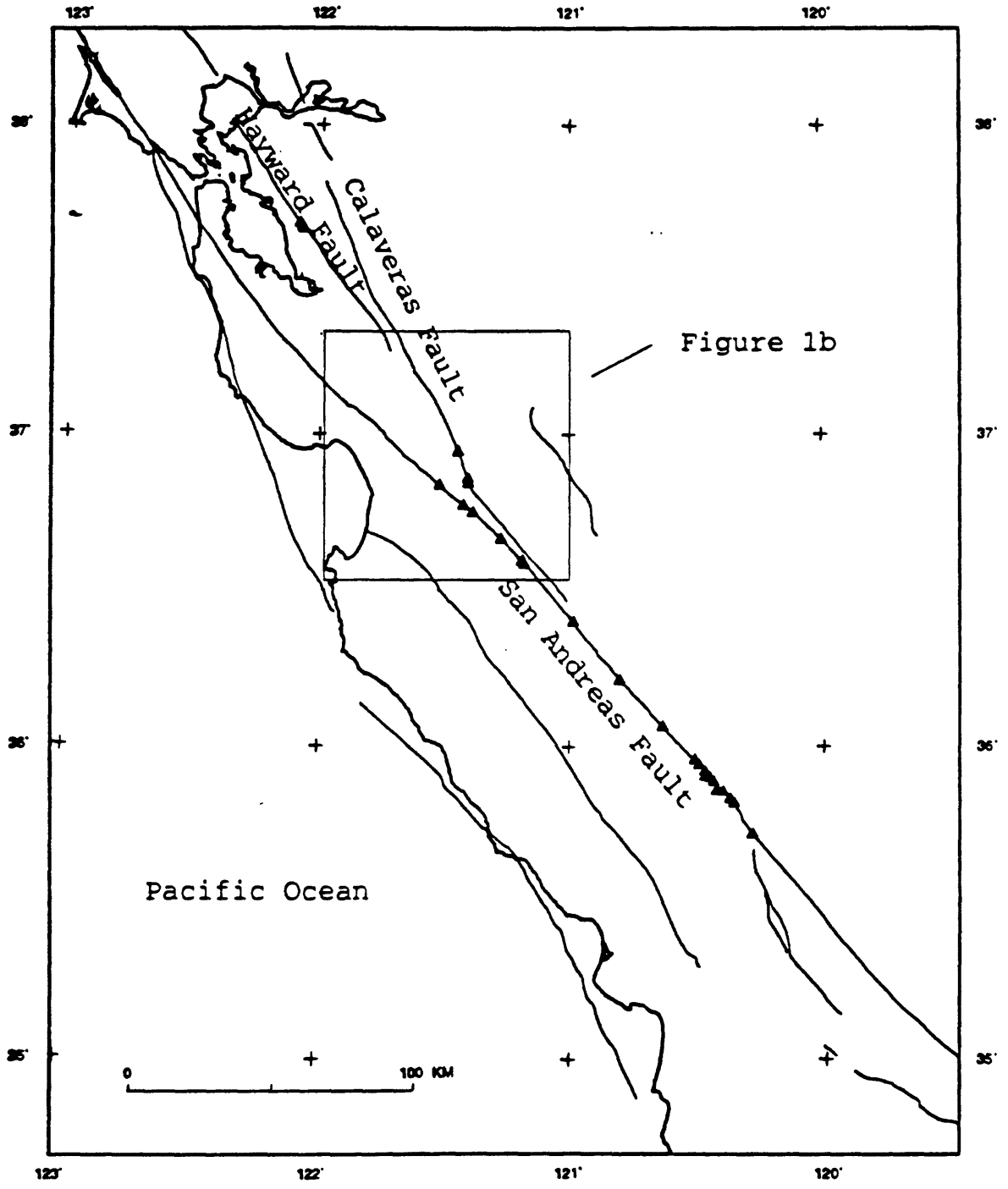

FIGURE 1a. Locations of USGS creepmeters in Central California in operation at the time of the Loma Prieta earthquake.

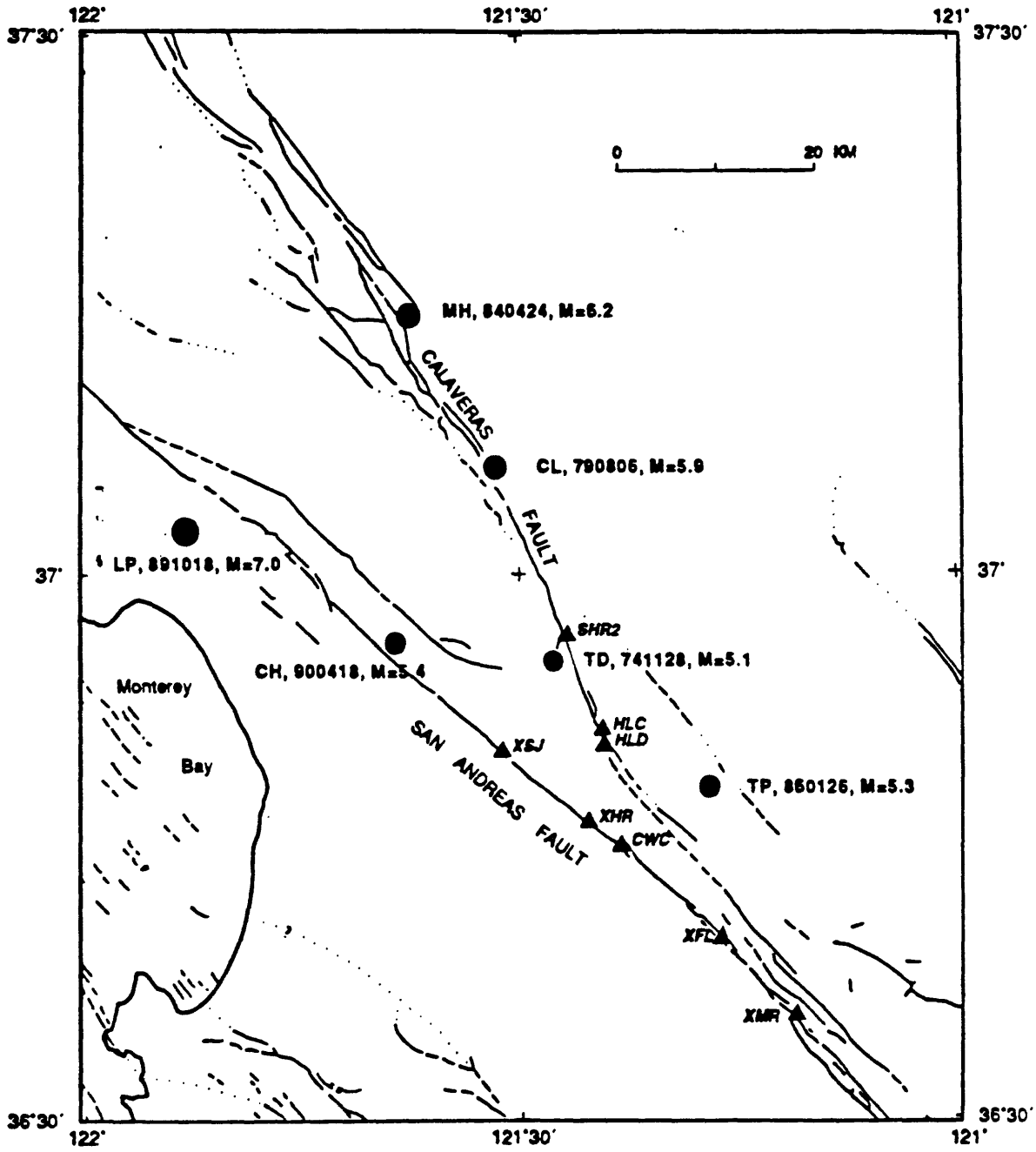

FIGURE 1b. Locations of 8 creepmeters discussed in the text lying within 60 km of the Loma Prieta rupture. Epicenters of six earthquakes discussed in the text are also shown.

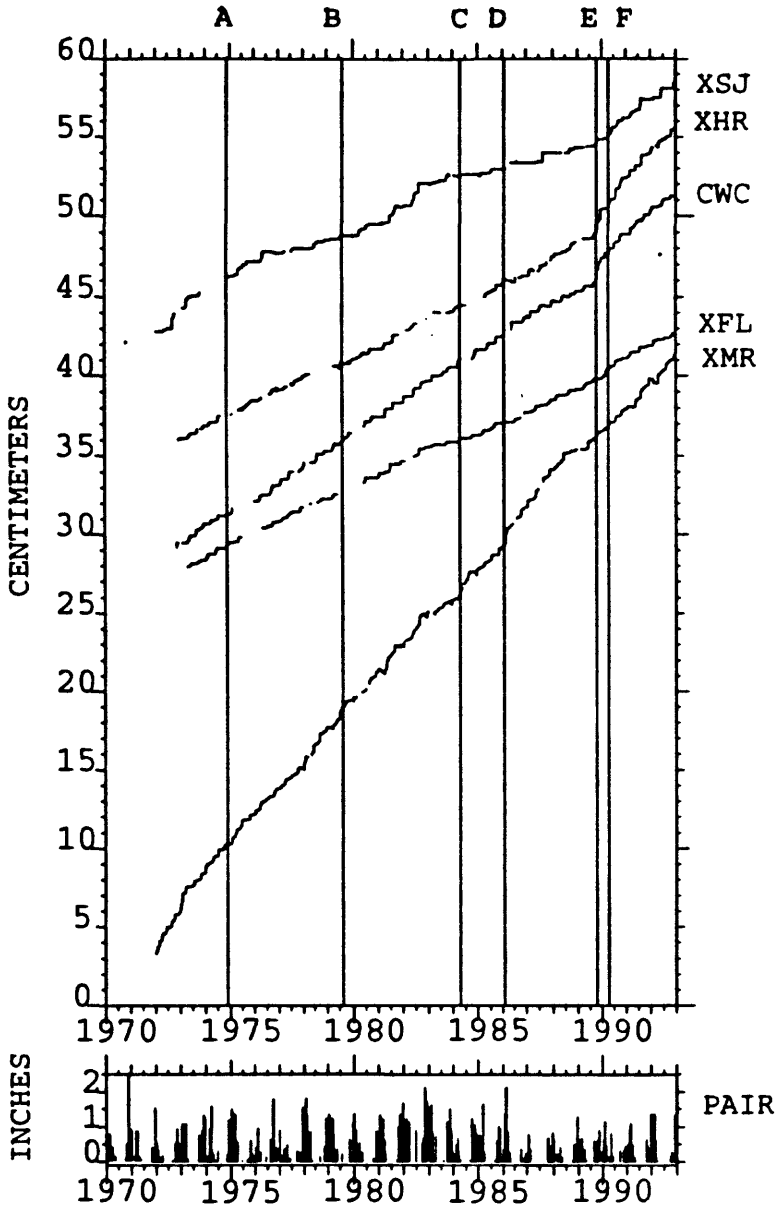

FIGURE 2a. Cumulative creep data for 5 creepmeters on the San Andreas fault from 1970 to 1993. Rainfall occurrences are also shown at the bottom of the plot. Vertical lines A through F mark the times of 6 moderate to large central California earthquakes discussed in the text and shown in Figure 1b.

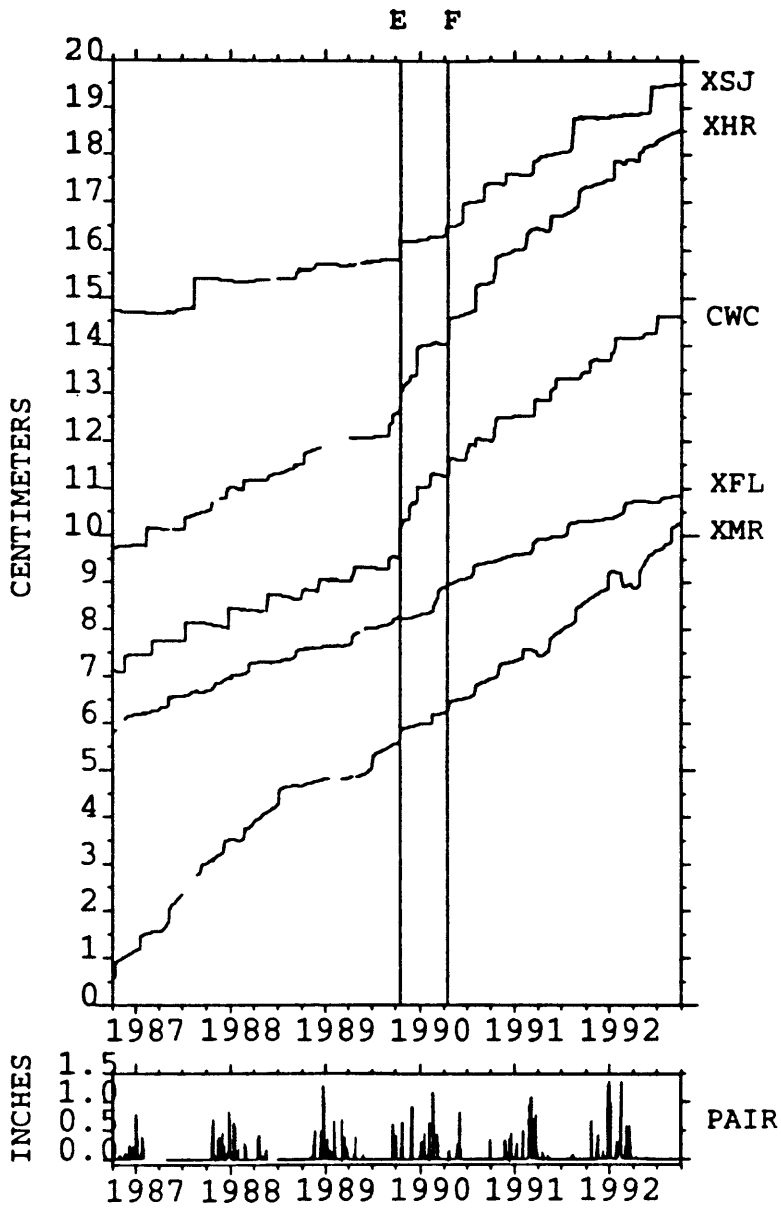

FIGURE 2b. Cumulative creep data for 5 creepmeters on the San Andreas fault from 3 years before to 3 years after the Loma Prieta earthquake. Rainfall occurrences are also shown at the bottom of the plot. Vertical lines E and F mark the times of the Loma Prieta earthquake and the Chittenden aftershock.

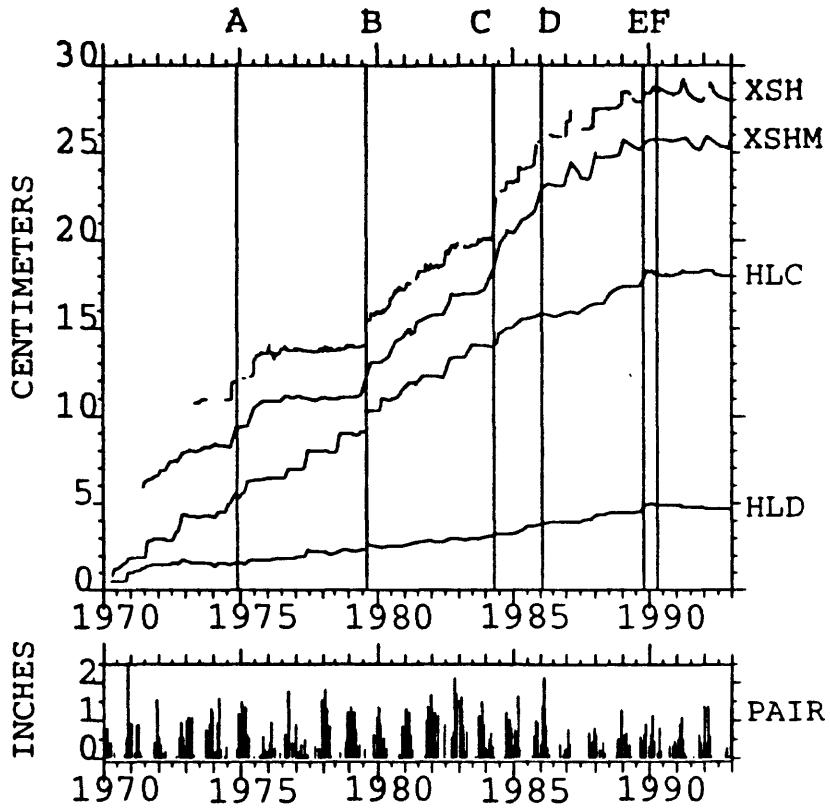

FIGURE 3a. Cumulative creep data for 3 creepmeters on the Calaveras fault from 1970 to 1993. XSHM is micrometer readings at site XSH, presented for easier comparison with the micrometer readings used for HLC and HLD. Rainfall occurrences are also shown at the bottom of the plot. Vertical lines A through F mark the times of 6 moderate to large central California earthquakes discussed in the text and shown in Figure 1b.

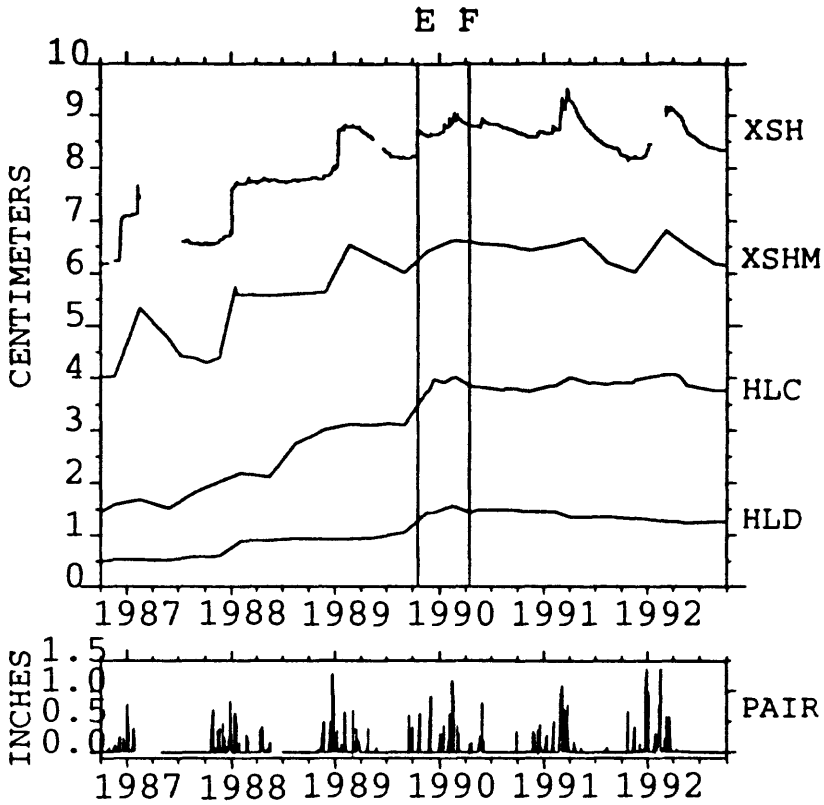

FIGURE 3b. Cumulative creep data for 3 creepmeters on the Calaveras fault from 3 years before to 3 years after the Loma Prieta earthquake. Trace XSHM represents quarterly micrometer readings at site XSH, presented for easier comparison with the dial gauge readings from HLC and HLD. Rainfall occurrences are also shown at the bottom of the plot. Vertical lines E and F mark the times of the Loma Prieta earthquake and the Chittenden earthquake.

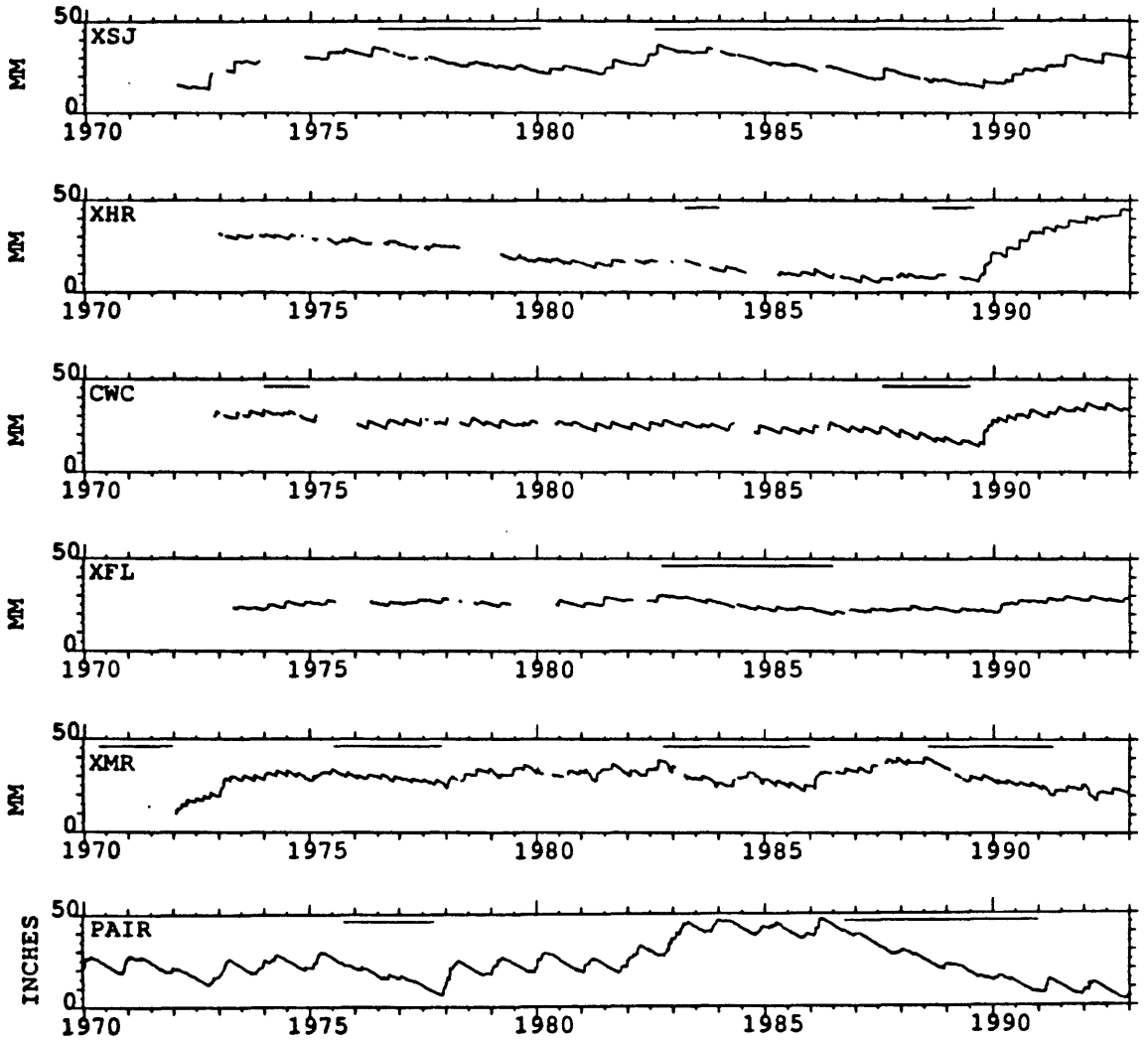

FIGURE 4a. Detrended creep data for 5 creepmeters on the San Andreas fault for 1970 to 1993. Trend was determined by calculating best-fitting least-squares line. Horizontal bars denote creep retardation. Bottom plot shows detrended cumulative rainfall record.

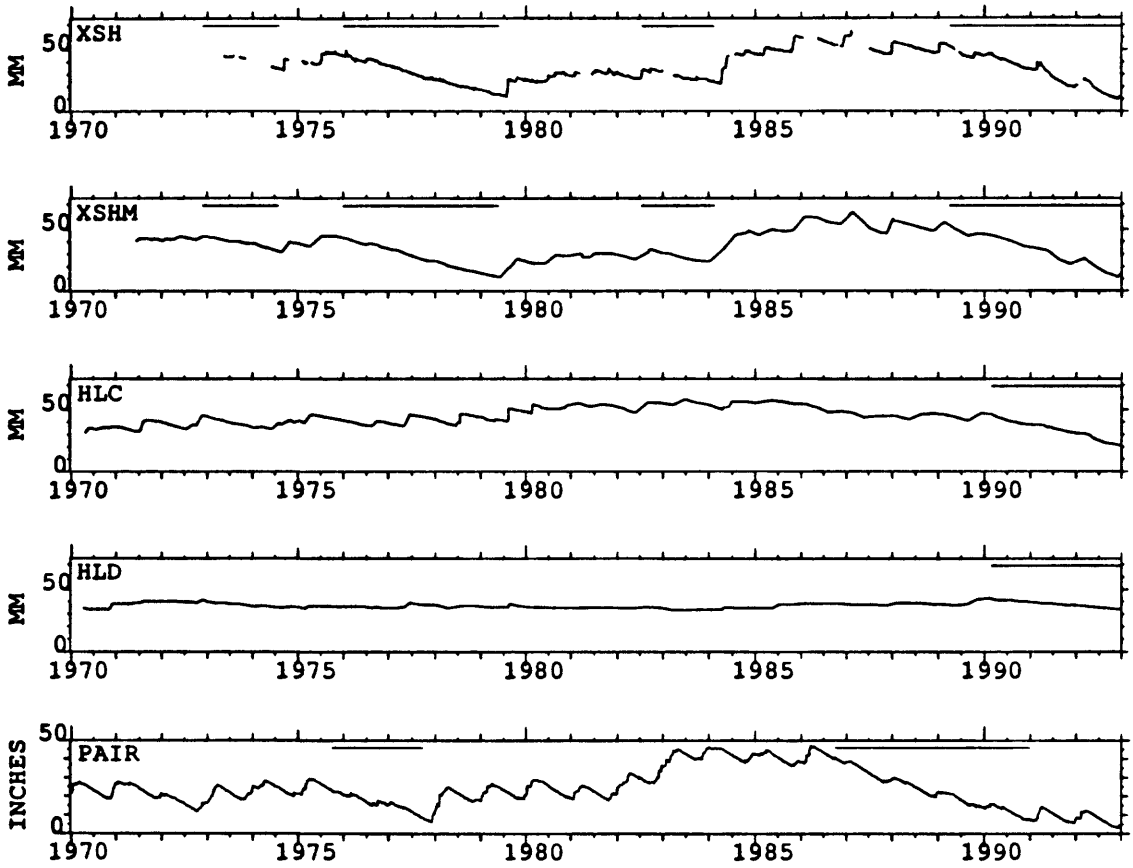

FIGURE 4b. Detrended creep data for 3 creepmeters on the Calaveras fault for 1970 to 1993. Trend was determined by calculating best-fitting least-squares line. XSHM is micrometer readings at site XSH, presented for easier comparison with the micrometer readings used for HLC and HLD. Horizontal bars denote creep retardation. Bottom plot shows detrended cumulative rainfall record.

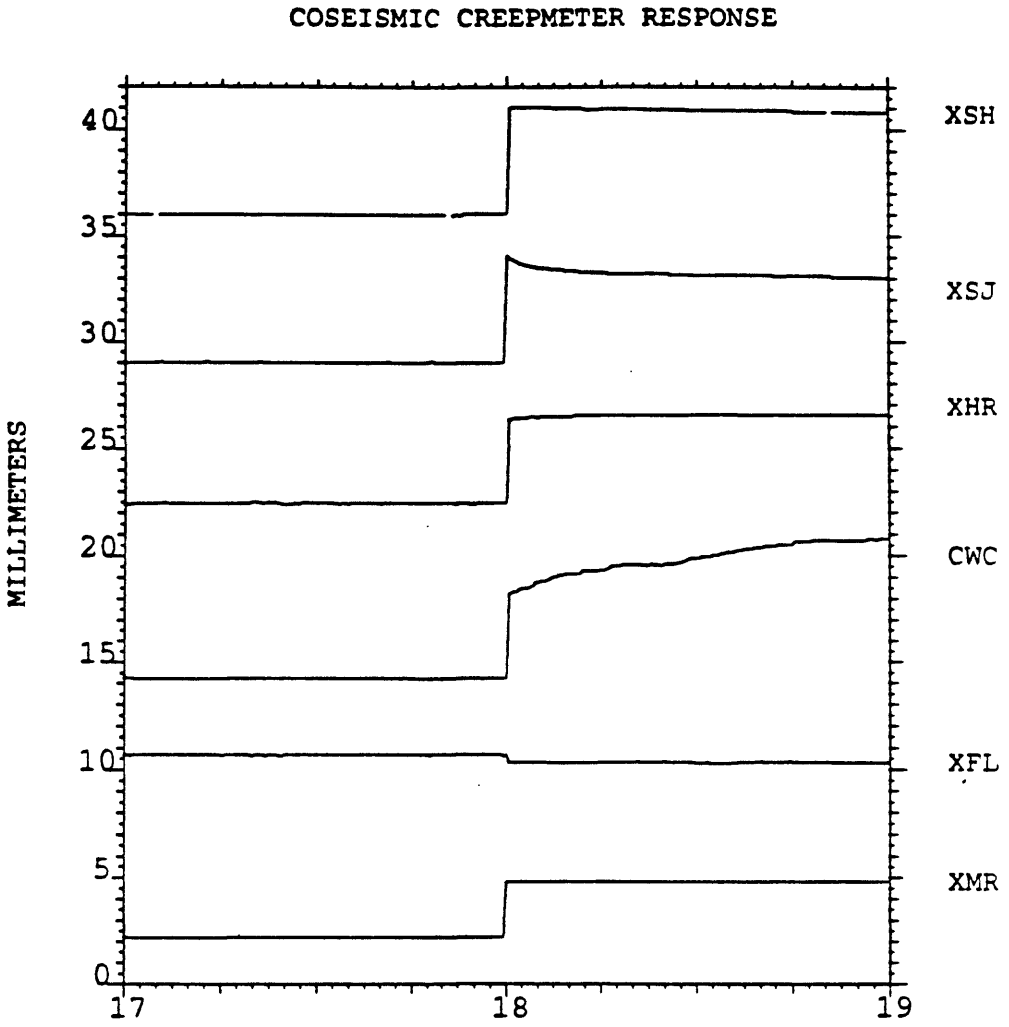

FIGURE 5. Coseismic response to the Loma Prieta earthquake for 6 creepmeters. XSH is on the Calaveras fault, while the others are on the San Andreas fault. Time extends from 2 days before to 2 days after the Loma Prieta earthquake.

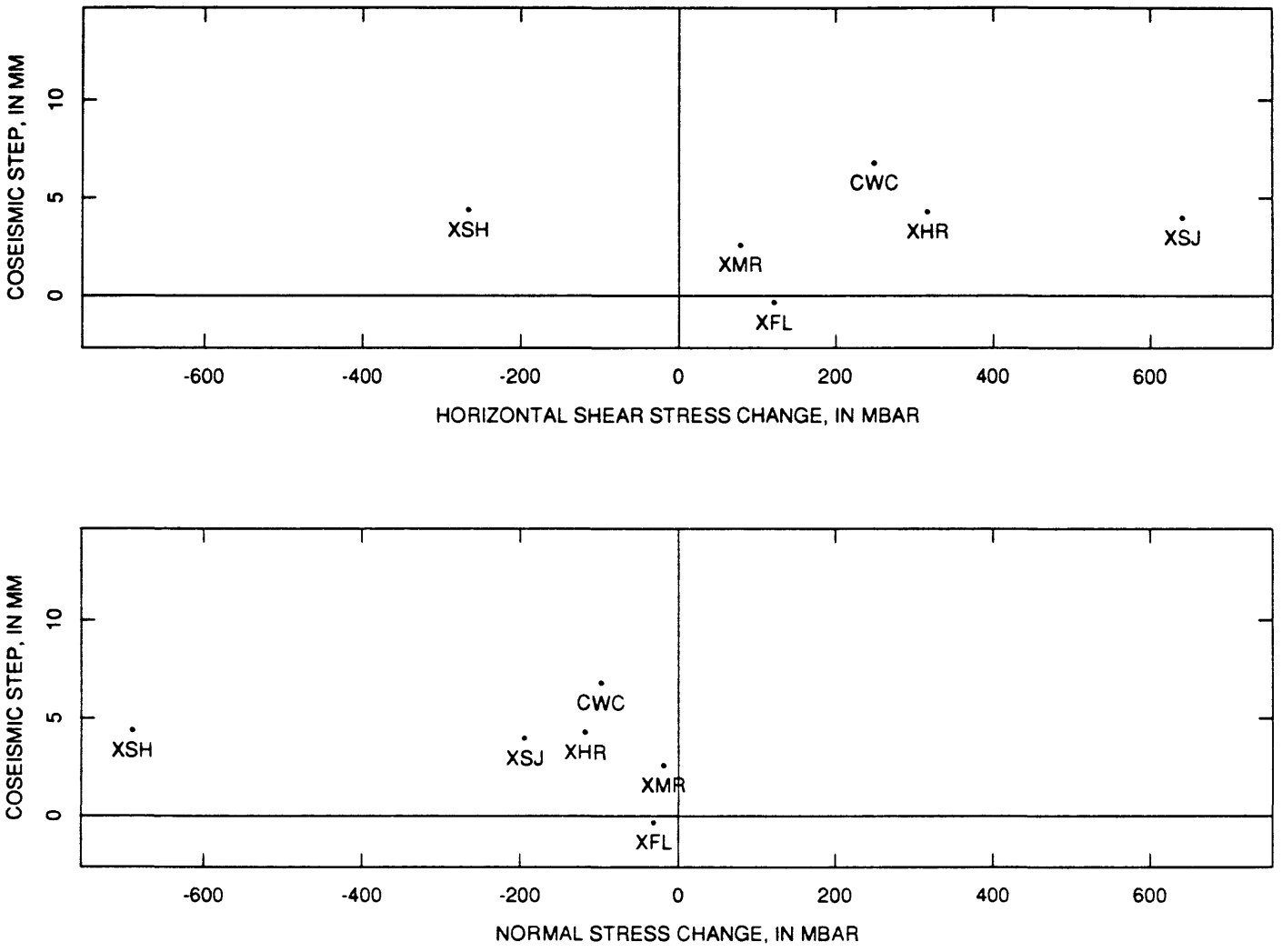

FIGURE 6. Coseismic steps for Loma Prieta earthquake at 6 creepmeters compared with calculated static stress changes. Coseismic steps are + for RL, -for LL. Shear stress is horizontal component, + for RL, - for LL. Normal stress is perpendicular component, + for extension, - for compression.

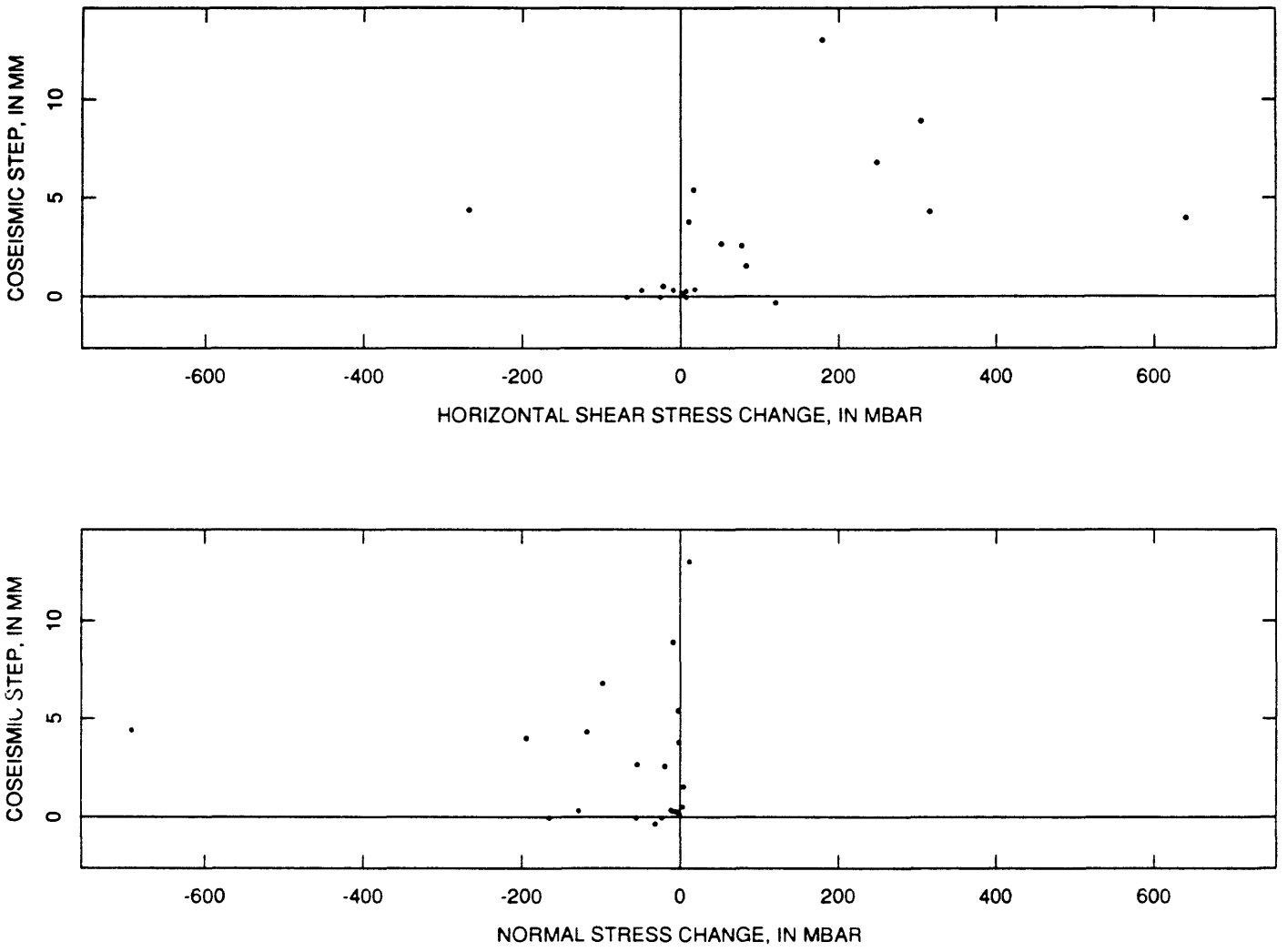

FIGURE 7. Coseismic steps for 6 earthquakes, including Loma Prieta earthquake, compared with calculated static stress changes. Sign conventions as in Figure 6.

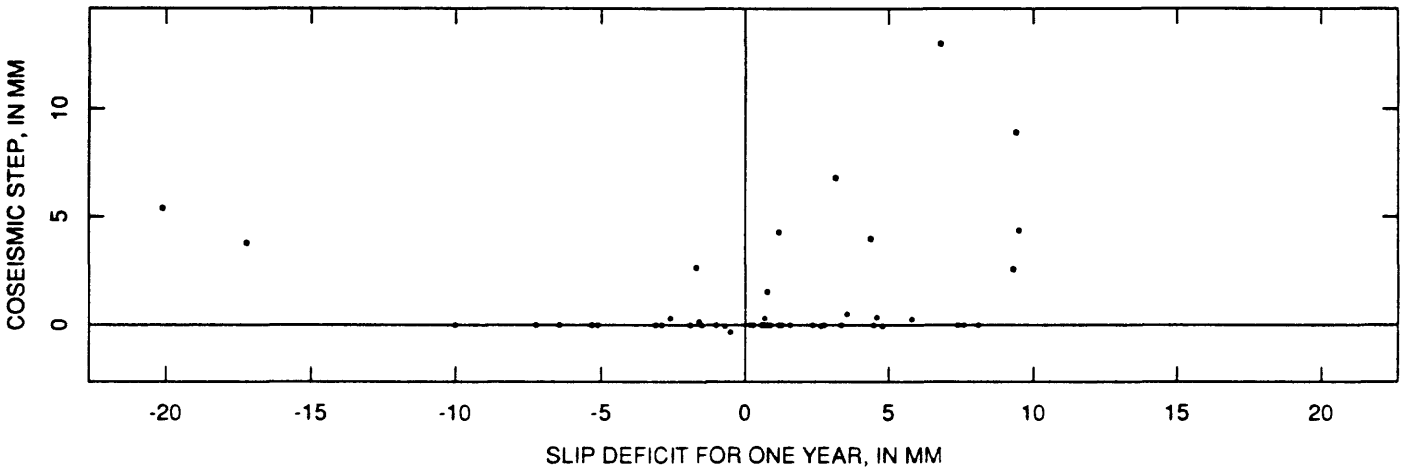

FIGURE 8. Coseismic steps for 6 earthquakes compared with 1-year slip deficit (defined as difference between the long term rate and the 1-year average rate prior to the earthquake).

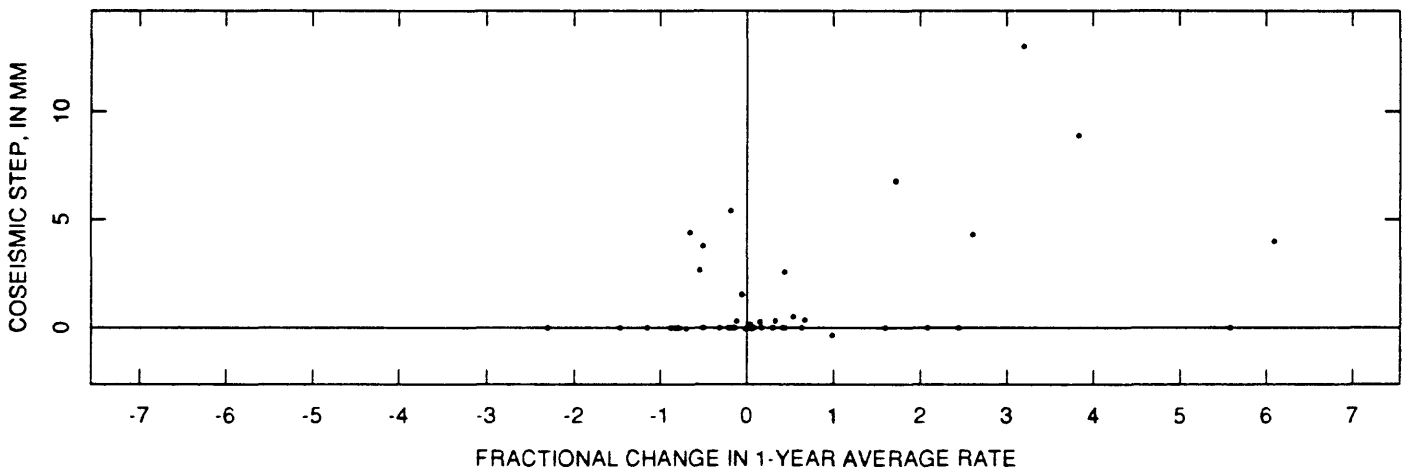

FIGURE 9. Coseismic steps for 6 earthquakes compared with fractional change in 1-year average creep rates. Fractional change is defined to be the 1-year average rate before the earthquake minus the 1-year average rate after the earthquake, divided by the 1-year average rate before the earthquake.

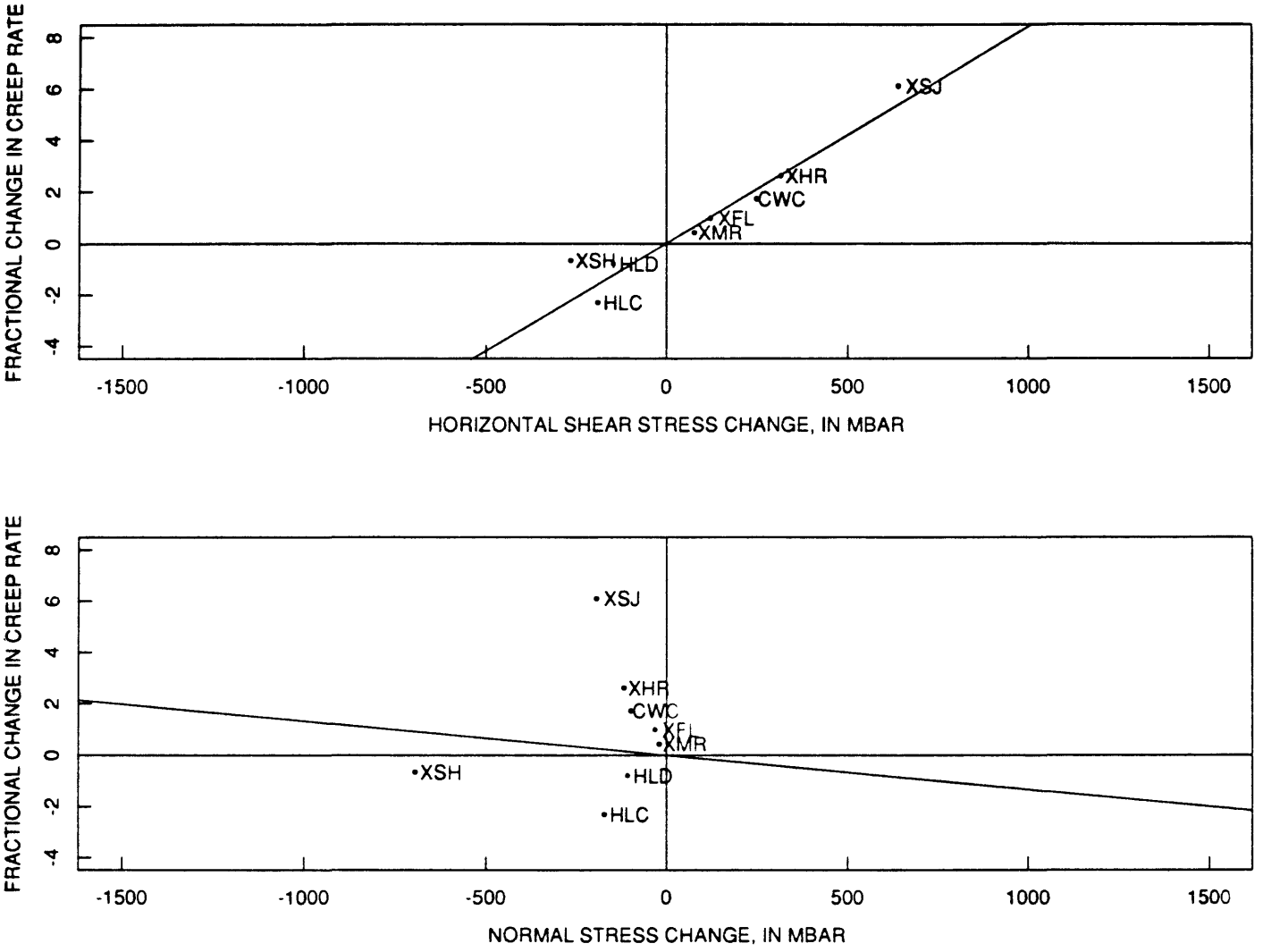

FIGURE 10a

FIGURE 10. Comparison of the fractional change in 1-year average creep rate at the time of Loma Prieta earthquake with calculated static stress changes for the 3 Loma Prieta slip distributions: (a) Lisowski and others (1990), (b) Marshall and others (1991), (c) Beroza (1991). Best fit line passing through the origin is also shown (see Table 4 for slopes).

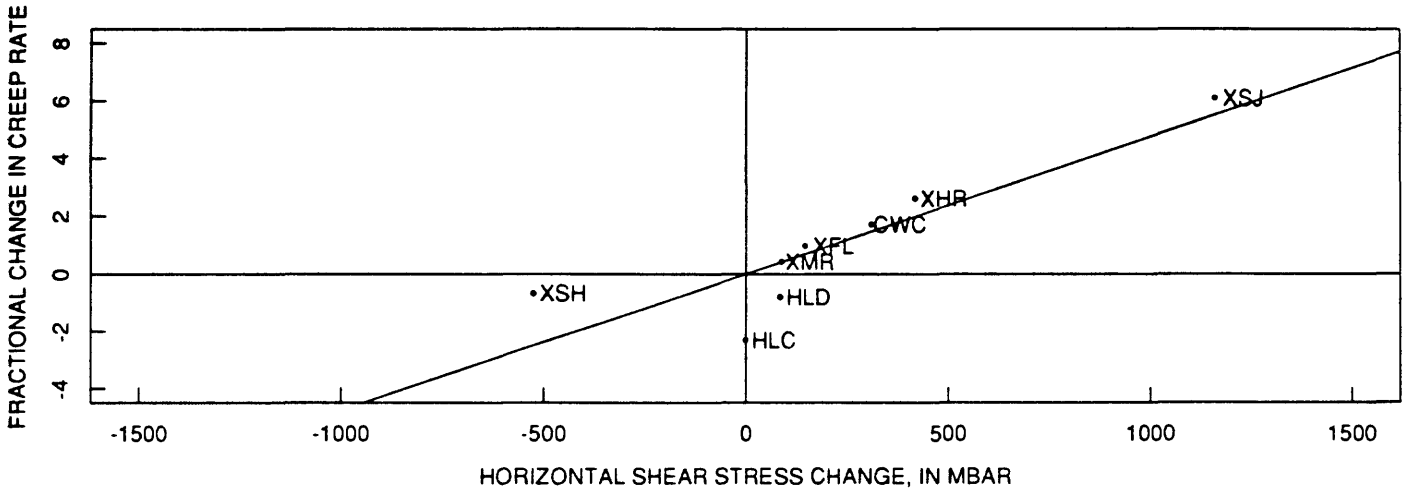
FRACTIONAL CHANGE IN CREEP RATE
8
6
4
2
0
-2
-4
XSJ
XHR
CWC
XFL
XMR
XSH
HLD
HLC
-1500
-1000
-500
0
500
1000
1500
HORIZONTAL SHEAR STRESS CHANGE, IN MBAR

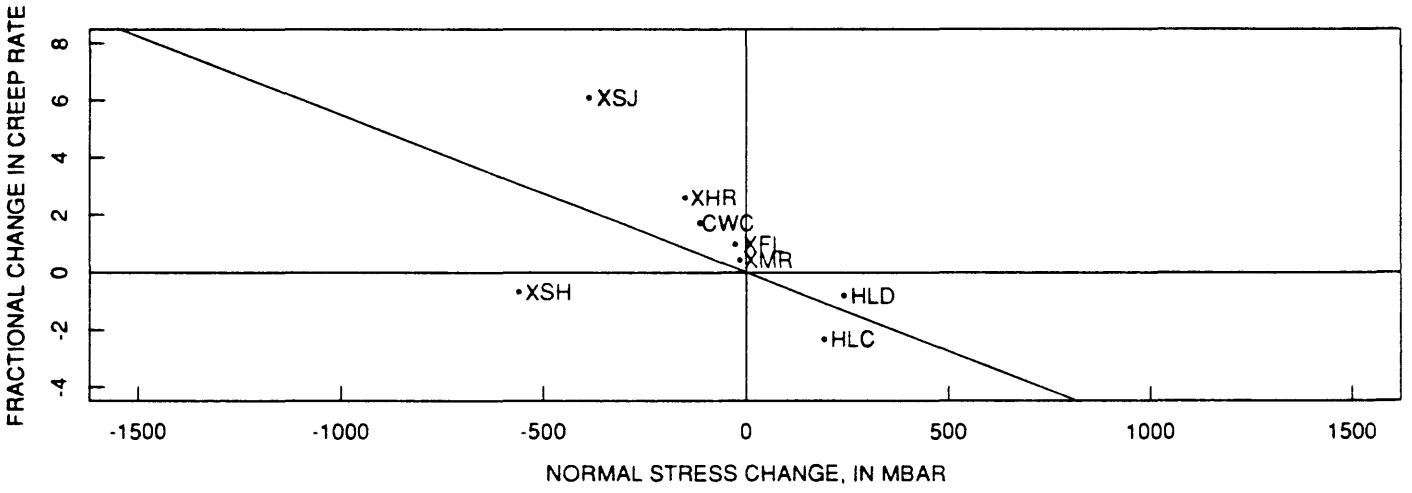
FRACTIONAL CHANGE IN CREEP RATE
8
6
4
2
0
-2
-4
XSJ
XHR
CWC
XFL
XMR
XSH
HLD
HLC
-1500
-1000
-500
0
500
1000
1500
NORMAL STRESS CHANGE, IN MBAR

FIGURE 10b

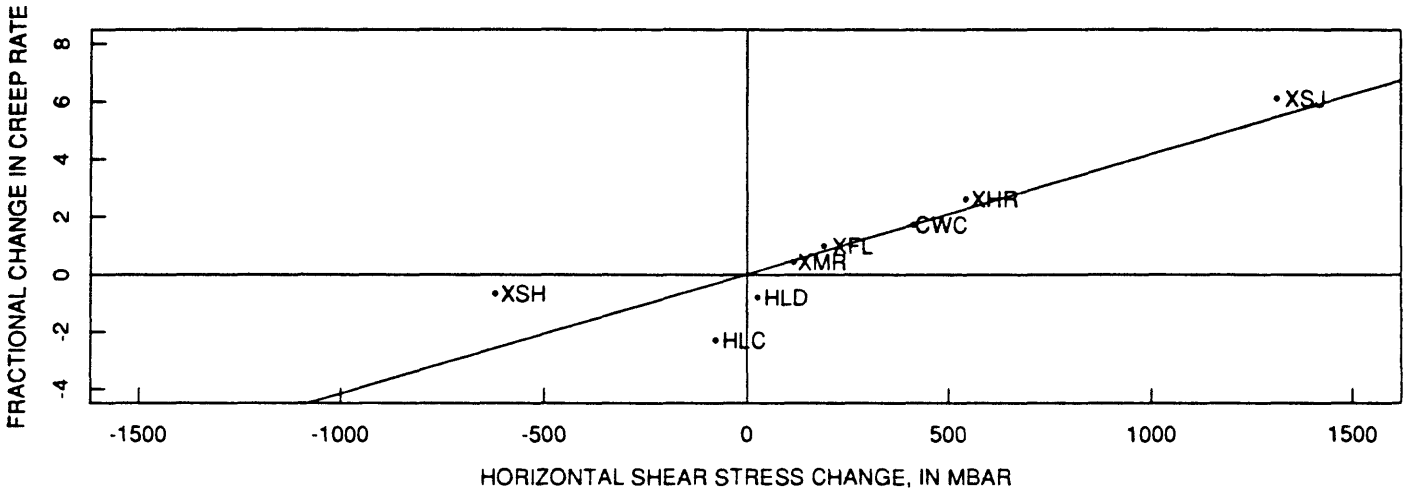
FRACTIONAL CHANGE IN CREEP RATE
8
6
4
2
0
-2
-4
XSJ
XHR
CWC
XFL
XMR
XSH
HLD
HLC
-1500
-1000
-500
0
500
1000
1500
HORIZONTAL SHEAR STRESS CHANGE, IN MBAR

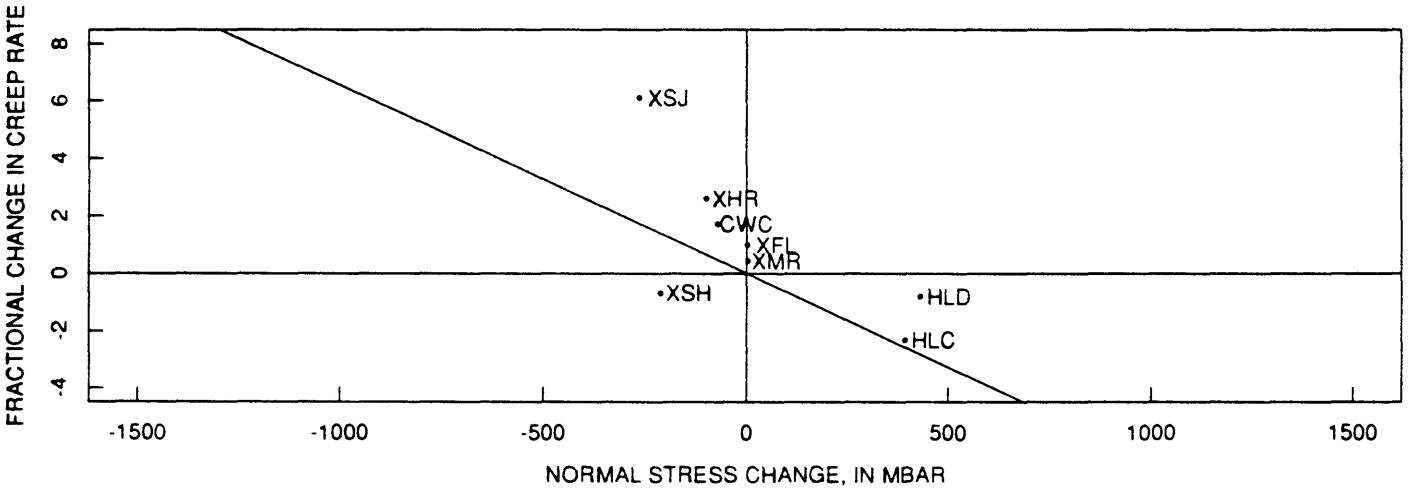
FRACTIONAL CHANGE IN CREEP RATE
8
6
4
2
0
-2
-4
XSJ
XHR
CWC
XFL
XMR
XSH
HLD
HLC
-1500
-1000
-500
0
500
1000
1500
NORMAL STRESS CHANGE, IN MBAR

FIGURE 10c

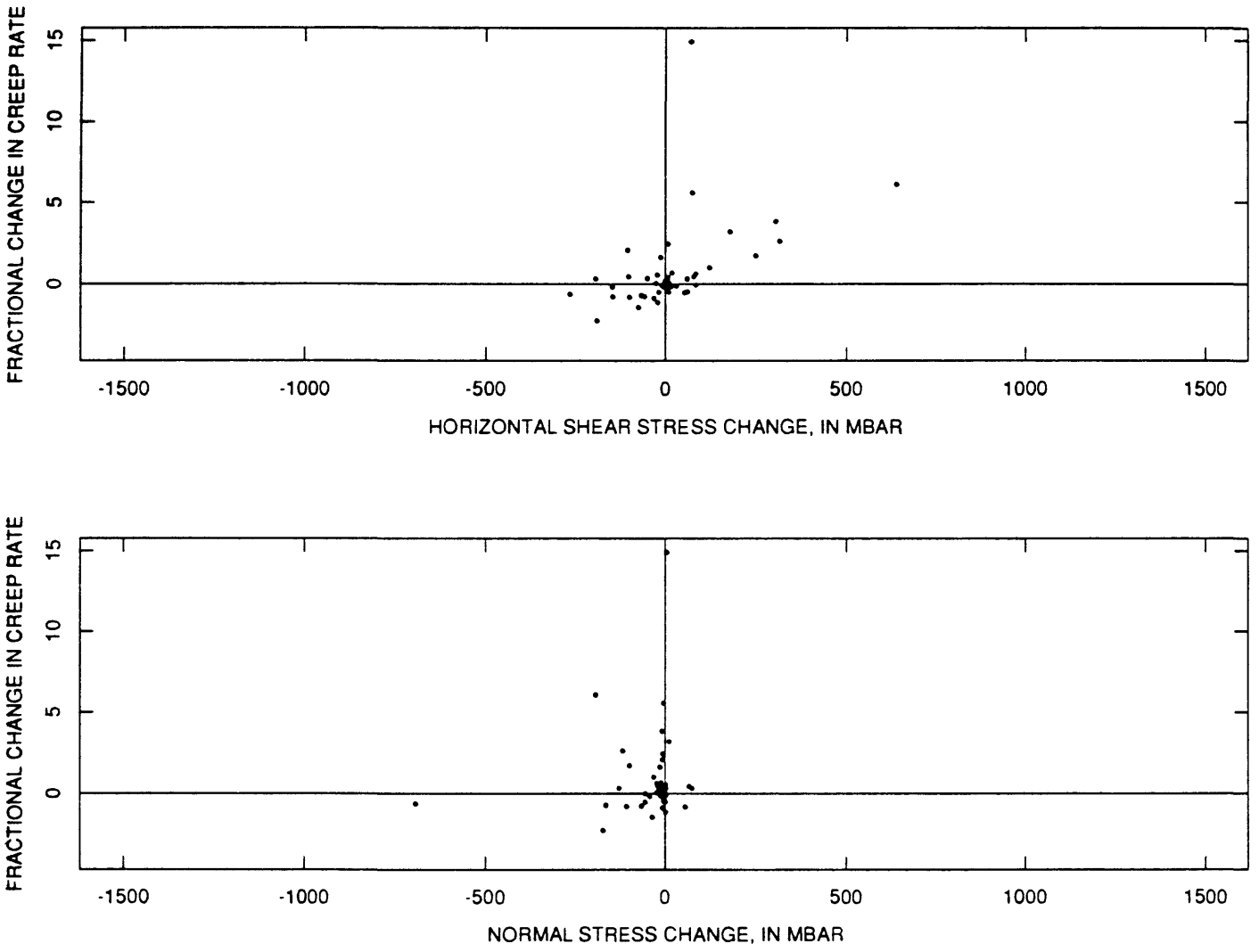

FIGURE 11. Comparison of the fractional change in 1-year average creep rate at the times of six earthquakes with calculated static stress changes for simple dislocation models of the earthquakes.

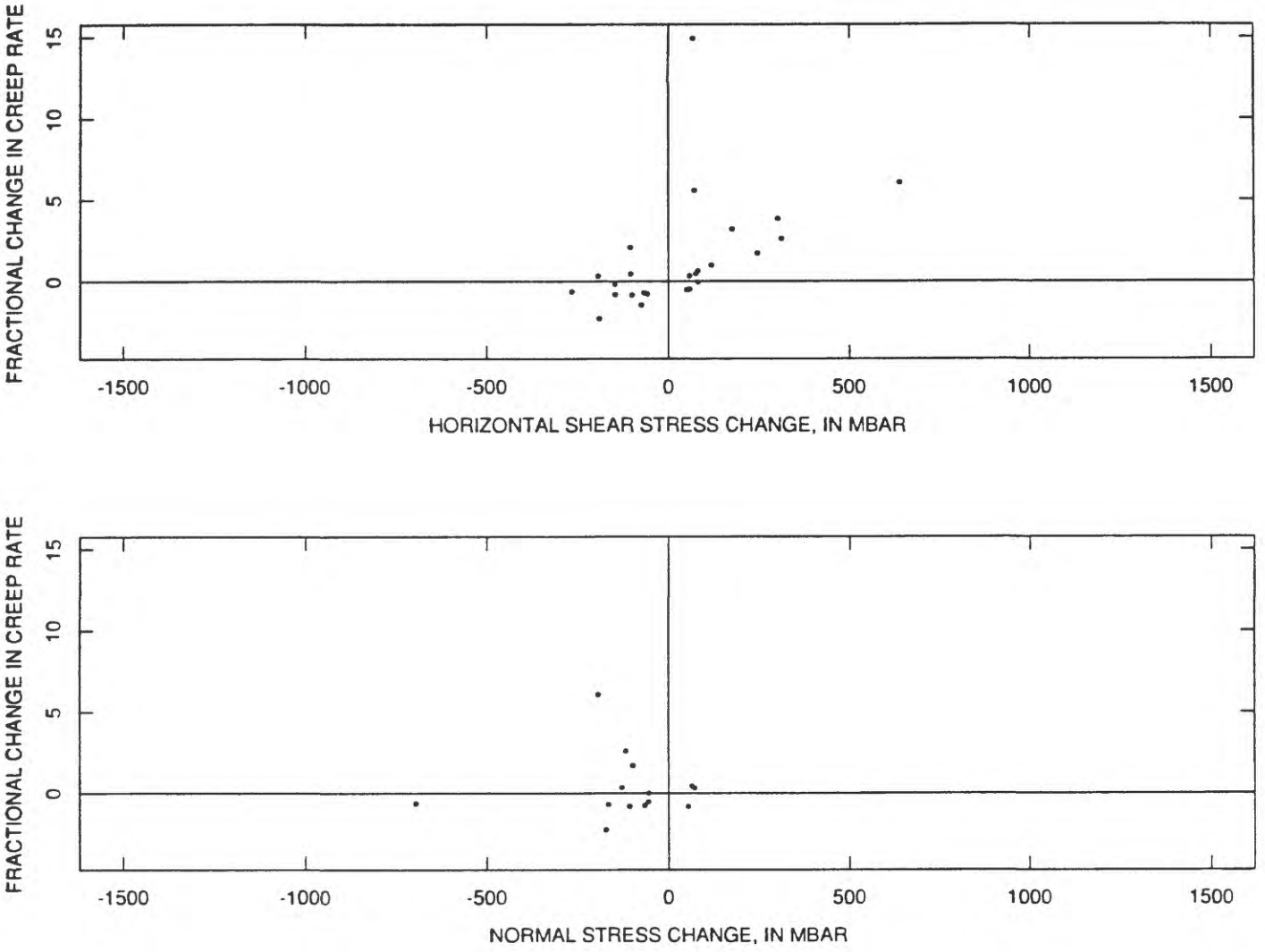

FIGURE 12. Comparison of the fractional change in 1-year average creep rate at the times of six earthquakes with calculated static stress changes greater than 0.05 bars in amplitude for simple dislocation models of the earthquakes.

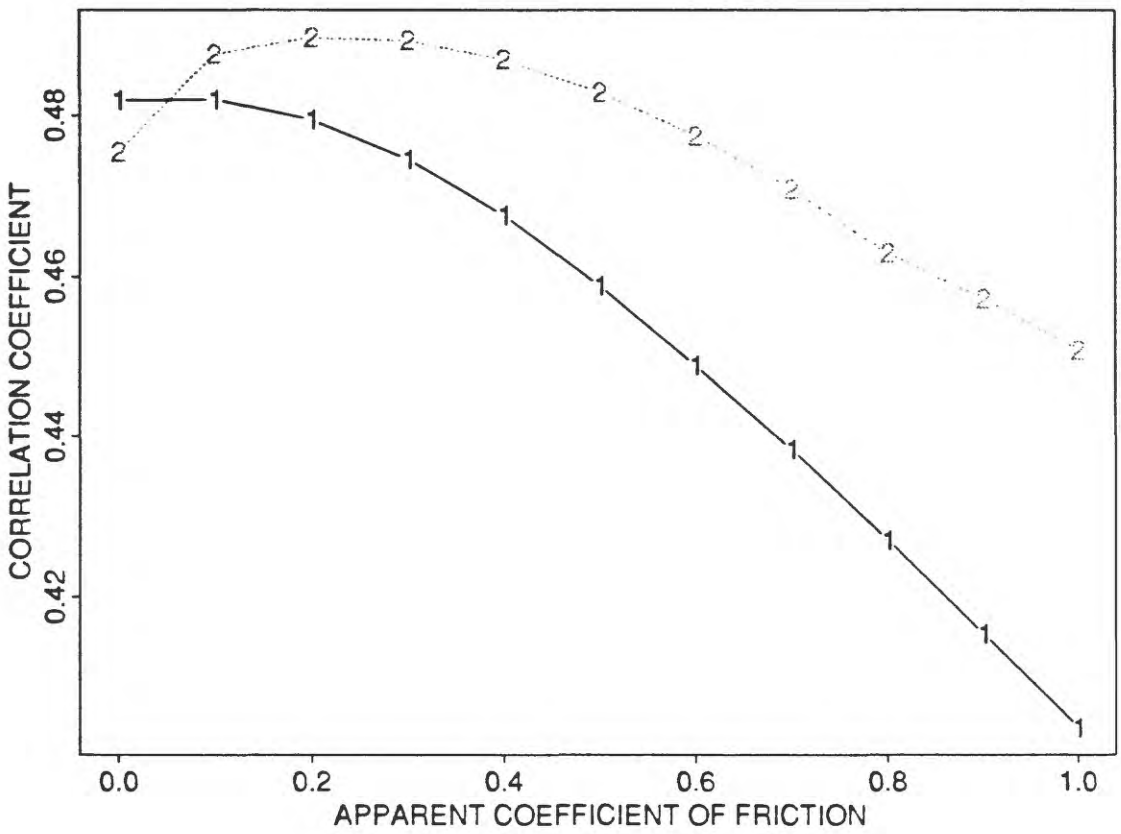

FIGURE 13. Correlation coefficient as a function of apparent coefficient of friction for correlation of fractional changes in 1-year creep rates with calculated shear stress change. Curve 1 represents results for all data. Curve 2 is for data with Coulomb failure function values greater than or equal to 0.05 bars.

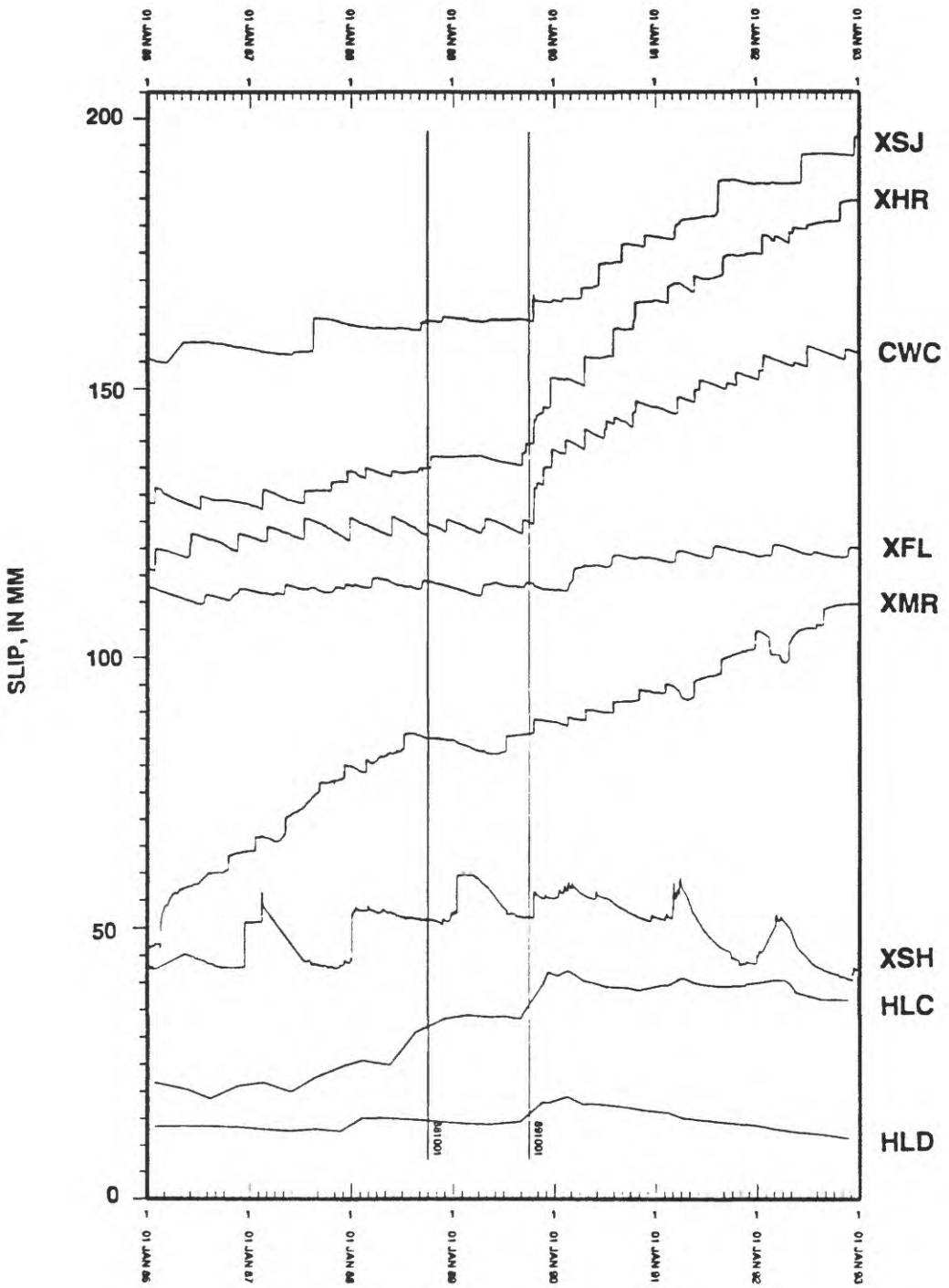

FIGURE 14. Plots of the Loma Prieta perturbation for 8 creepmeters with 1-year average rates for the year before the Loma Prieta earthquake subtracted to enhance the perturbations.

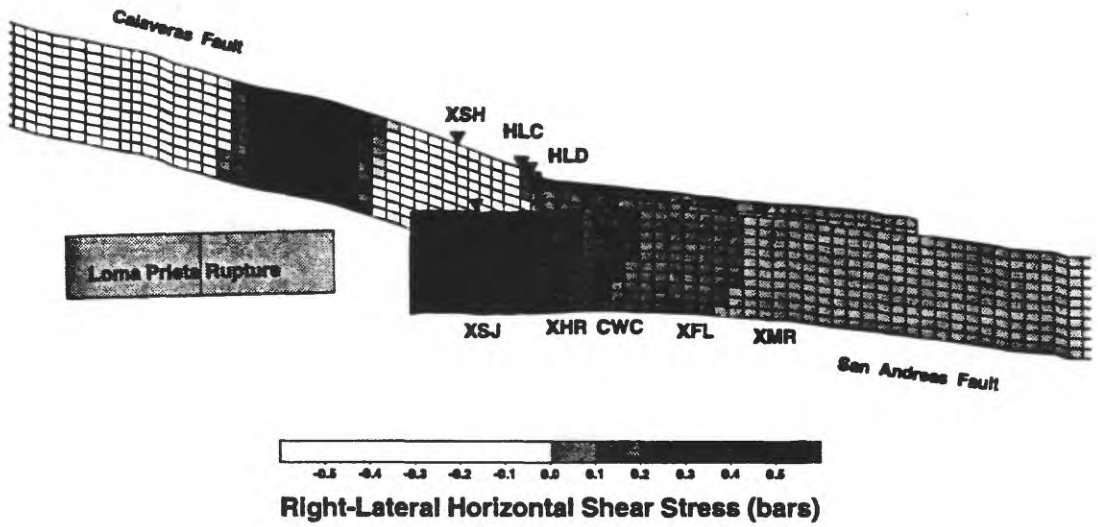

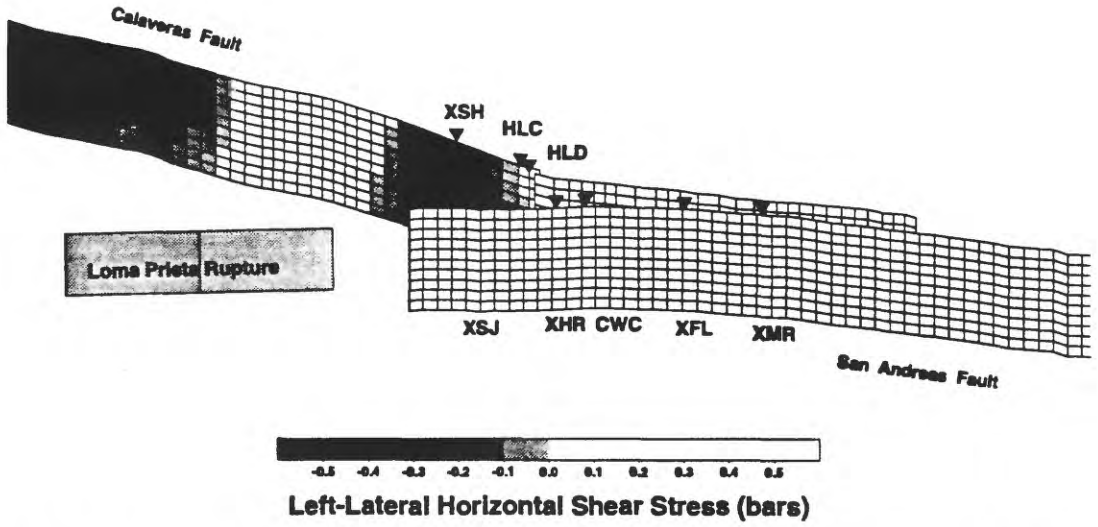

FIGURE 15. Oblique view from the southwest, showing geometry of one dislocation model used to calculate Loma Prieta stress changes and resulting anomalous displacements. San Andreas fault south of the Loma Prieta rupture is in the foreground and the Calaveras fault in the background, In the top figure, gray shading indicates increased (RL) horizontal shear stress calculated using Marshall and others (1990) slip distribution. In the bottom figure, shading indicates decreased (LL) horizontal shear stress. Each small rectangle is approximately 2-km by 2-km in size. The fault planes in this model extend vertically to a depth of 20 km. Locations of creepmeters discussed in the text are shown.

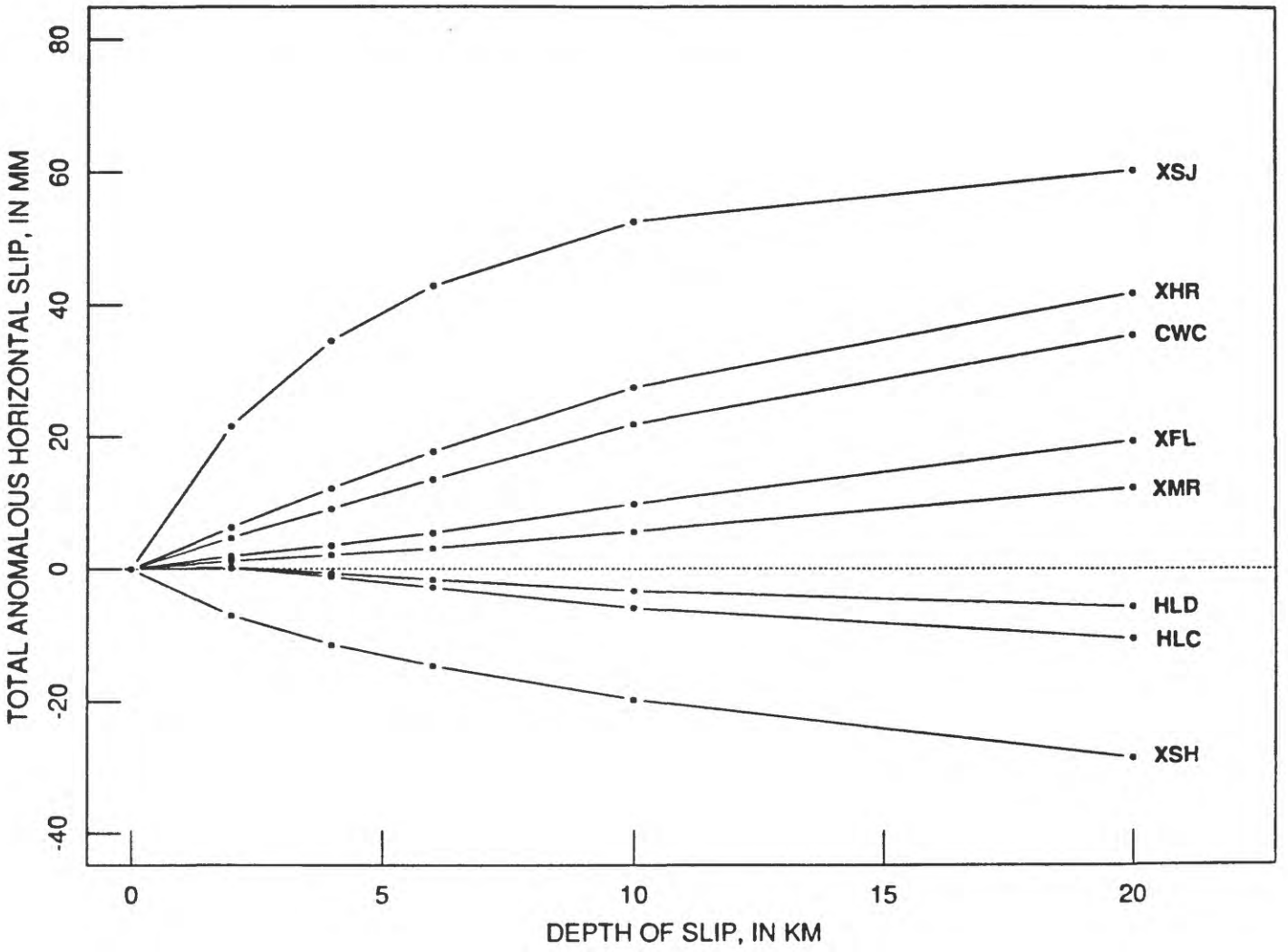

FIGURE 16. Plot of total post-Loma Prieta anomalous slip predicted at eight creepmeter sites as a function of the depth to the bottom of the freely-slipping layer in model.

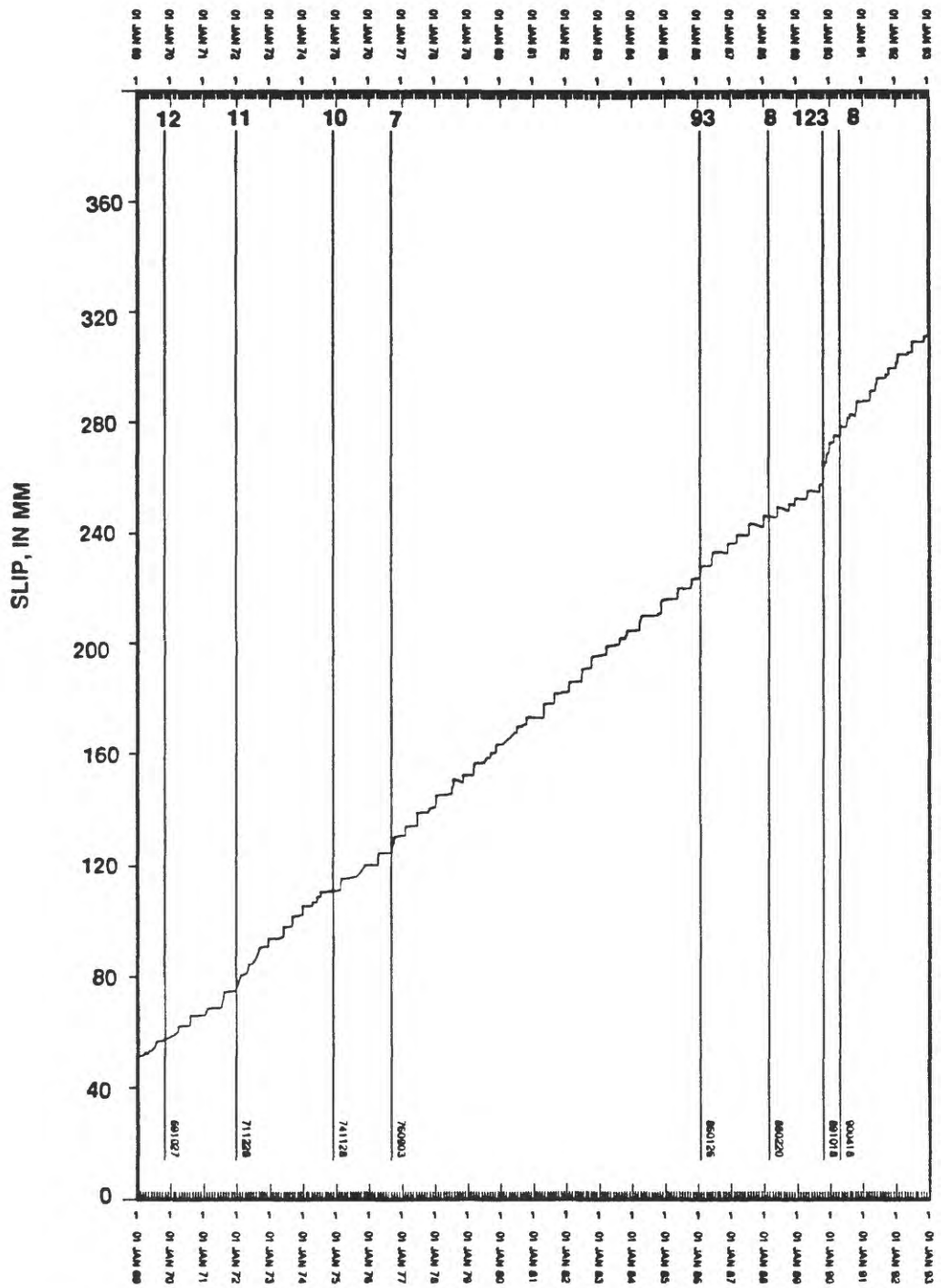

FIGURE 17. Plot of creep record for CWC showing times of earthquakes that might have had an effect at this site. Earthquakes were selected from the CALNET catalog by scaling their moment by d^{-3} which is the fall-off of maximum stress from a point dislocation, disregarding orientation. Numbers at tops of lines compare potential impact of the earthquake's static stresses (without regard to orientation information - so the value is an upper bound) to the impact expected from an optimally oriented magnitude 4 earthquake at a distance of 10 km.

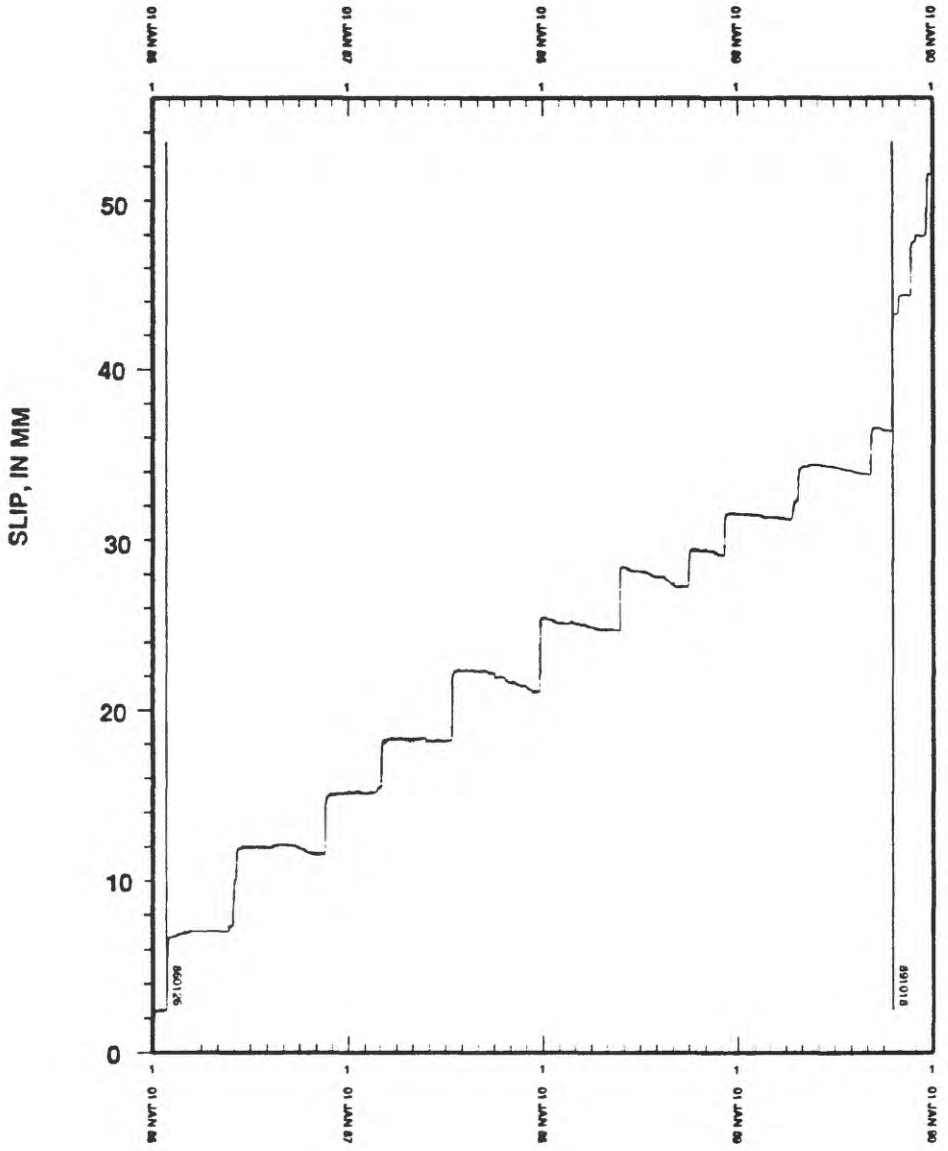

FIGURE 18. CWC creep record from 1983-1989 showing pre-Loma Prieta retardation begining in 1987, with the times of the Tres Pinos and Loma Prieta earthquakes.

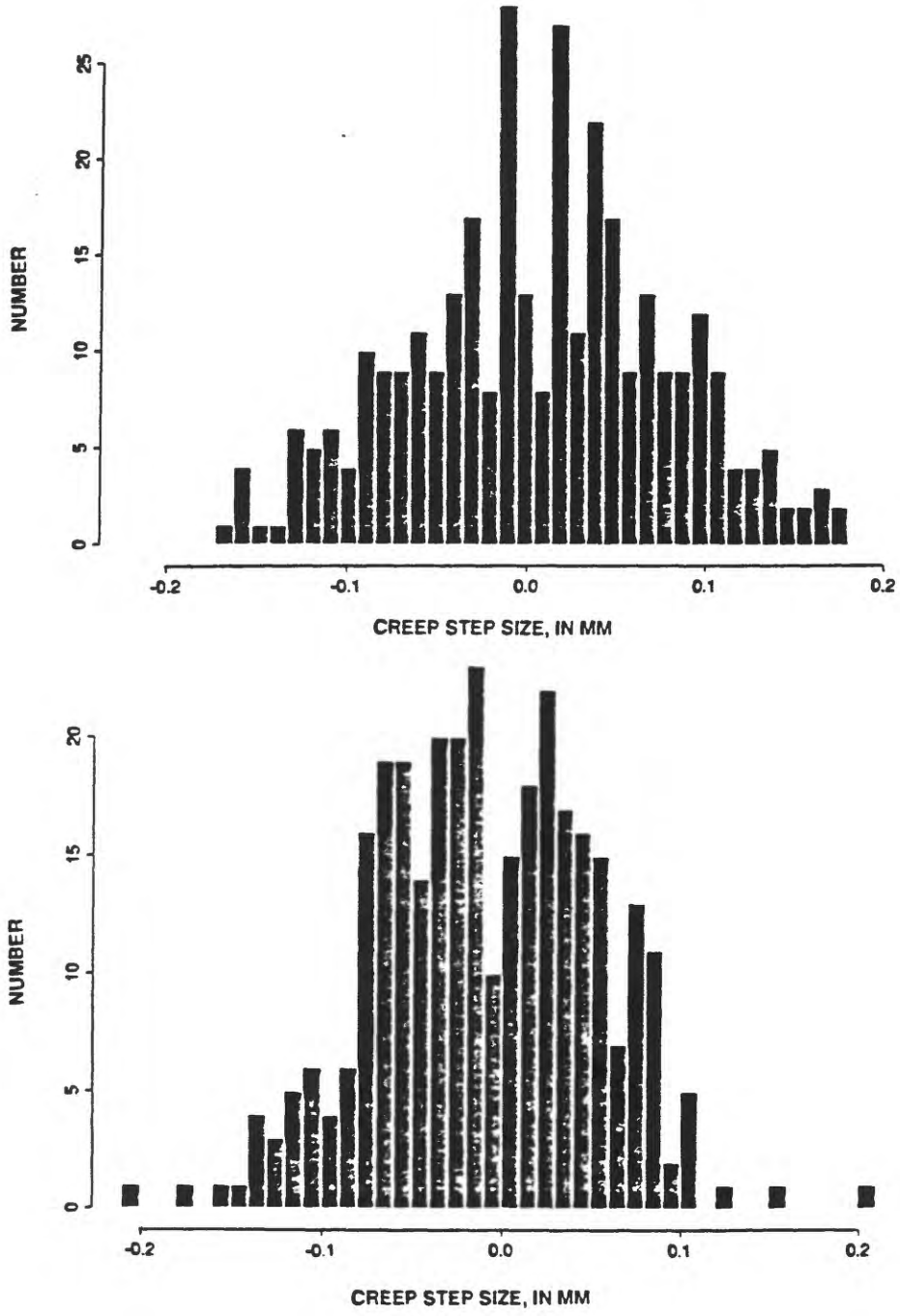

FIGURE 19. Histogram of creep step sizes smaller than 0.25 mm from daily data between 1 October 1987 and 1 October 1988 (bottom) compared with a similar histogram for the period from 1 January 1981 to 1 January 1982 (top).

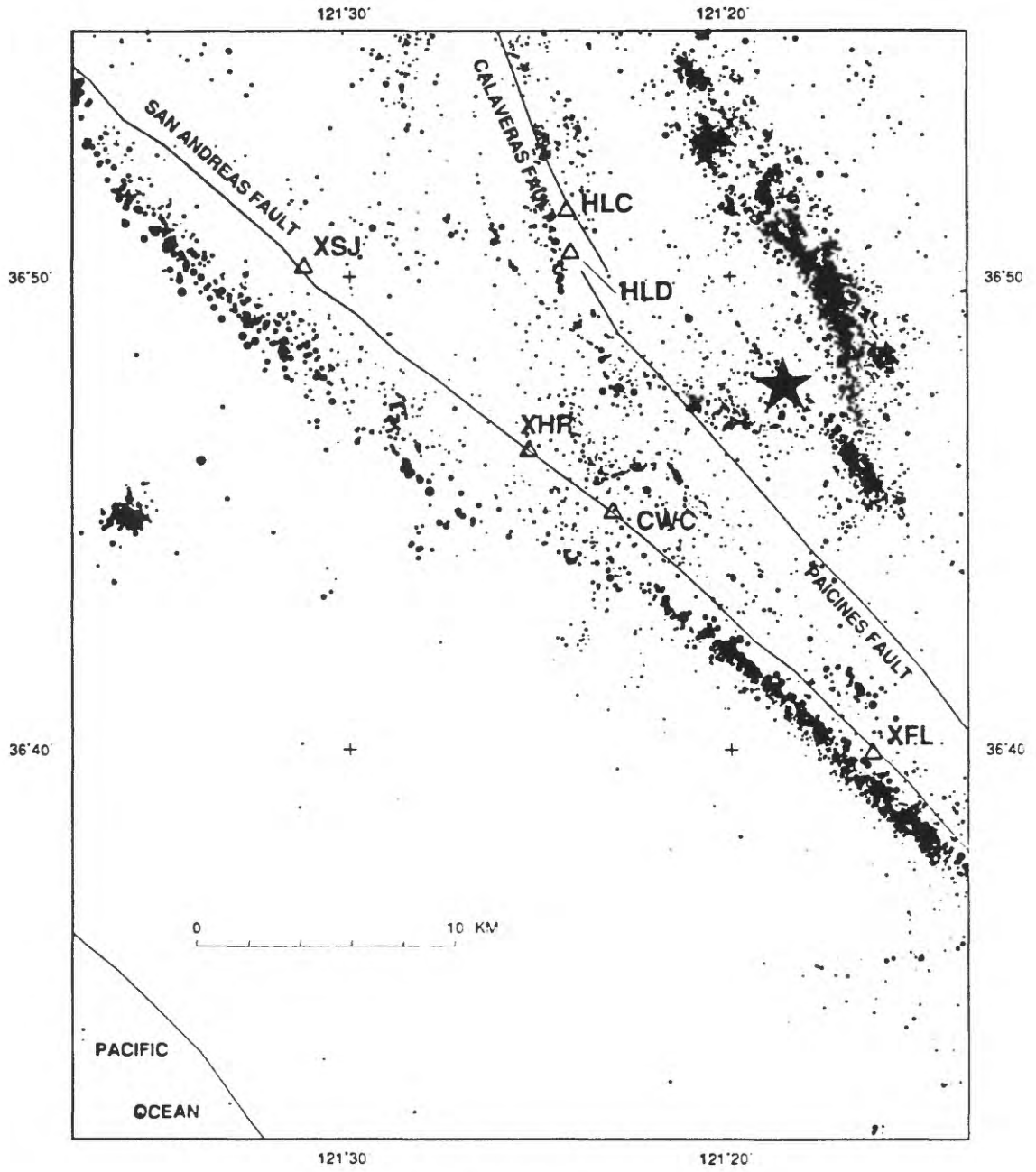

FIGURE 20a

FIGURE 20. (a) Earthquakes in the area of creepmeter CWC during the period from 1983-1988 from the CALNET catalog. (b) Earthquakes for the same area from 1 January 1987 to 1 September 1988 during the period of retardation observed on creepmeter CWC when left-lateral steps were most obvious. Earthquakes do not lie exactly under the fault traces, probably in part because of deficiencies in the velocity models and in part because the faults may not be vertical. A star marks the epicenter of the January 26, 1986 Tres Pinos earthquake.

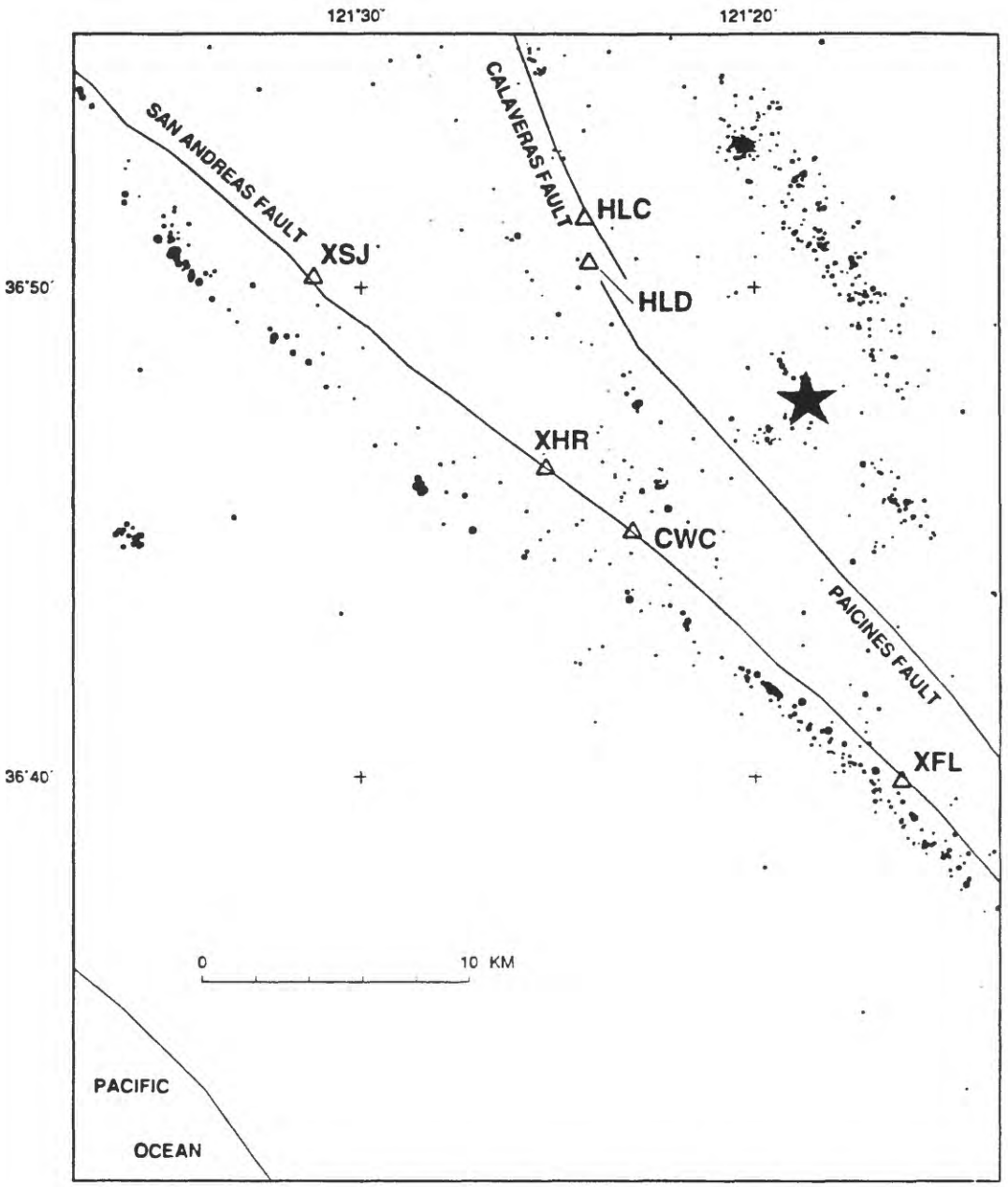
121°30'
121°20'
36°50'
36°40'
SAN ANDREAS FAULT
CALAVERAS FAULT
PAICINES FAULT
XSJ
HLC
HLD
XHR
CWC
XFL
0
10 KM
PACIFIC
OCEAN

FIGURE 20b

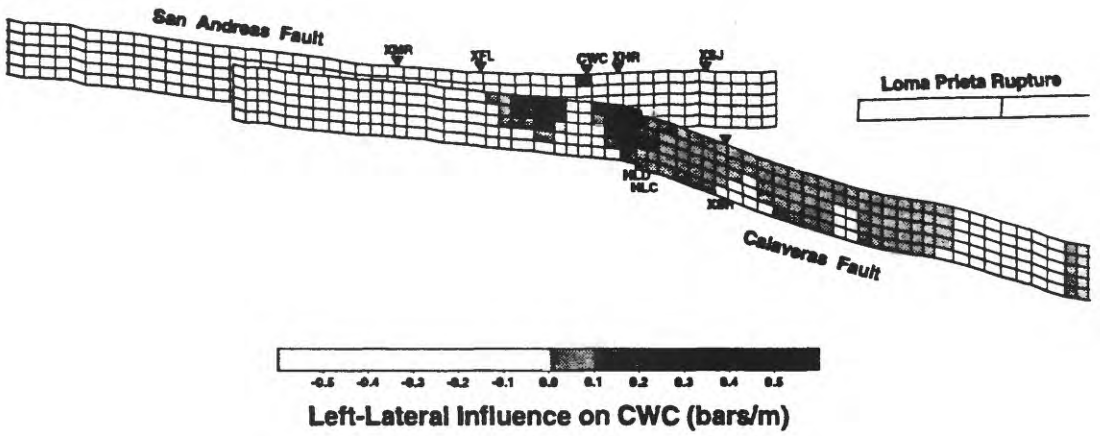

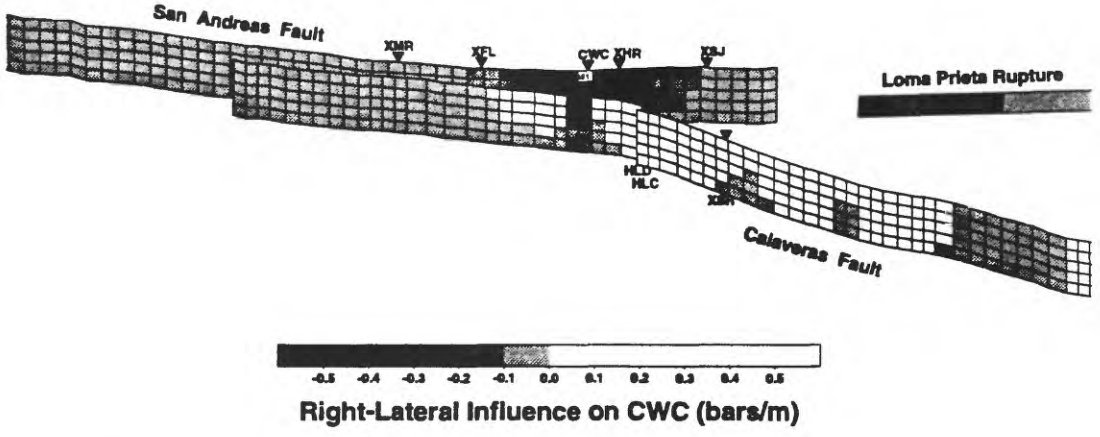

FIGURE 21. Oblique view from the northeast with the Calaveras fault in the foreground and the San Andreas fault in the background, showing influence coefficients relative to rectangular patch under creepmeter CWC. In the top figure, gray shaded regions indicate fault patches where RL slip would induce LL stress change at CWC. In the bottom figure, shaded regions indicate patches where RL slip would induce RL stress change at CWC. Note that on the parts of the San Andreas fault shown in the figure, LL slip would be required to produce LL stress at CWC, whereas on the Calaveras fault, there are regions where RL slip can produce LL stress at CWC. Each small rectangle is approximately 2-km by 2-km in size. The fault planes in this model extend vertically to a depth of 10 km.